The physics of the colloidal glass transition

2012 Rep. Prog. Phys. 75 066501

(http://iopscience.iop.org/0034-4885/75/6/066501)

Rep. Prog. Phys. **75** (2012) 066501 (30pp) doi:10.1088/0034-4885/75/6/066501

The physics of the colloidal glass transition

Gary L Hunter and Eric R Weeks

Department of Physics, Emory University, Math and Science Center 400 Dowman Dr., N201 Atlanta, GA 30322, USA

E-mail: weeks@physics.emory.edu

Received 26 June 2011, in final form 15 March 2012
Published 16 May 2012
Online at stacks.iop.org/RoPP/75/066501

Abstract

As one increases the concentration of a colloidal suspension, the system exhibits a dramatic increase in viscosity. Beyond a certain concentration, the system is said to be a colloidal glass; structurally, the system resembles a liquid, yet motions within the suspension are slow enough that it can be considered essentially frozen. For several decades, colloids have served as a valuable model system for understanding the glass transition in molecular systems. The spatial and temporal scales involved allow these systems to be studied by a wide variety of experimental techniques. The focus of this review is the current state of understanding of the colloidal glass transition, with an emphasis on experimental observations. A brief introduction is given to important experimental techniques used to study the glass transition in colloids. We describe features of colloidal systems near and in glassy states, including increases in viscosity and relaxation times, dynamical heterogeneity and ageing, among others. We also compare and contrast the glass transition in colloids to that in molecular liquids. Other glassy systems are briefly discussed, as well as recently developed synthesis techniques that will keep these systems rich with interesting physics for years to come.

(Some figures may appear in colour only in the online journal)

This article was invited by P Chaikin.

Contents

1. Introduction

1.1. What is the colloidal glass transition?

Imagine you have a bucket of ink. Ink is composed of colourful micrometre-sized particles in water. If you let the water evaporate from the ink, the ink becomes more and more viscous and at some point, it is still damp but no longer flows easily. This increase in viscosity as the water is removed is the colloidal glass transition, and in many respects is analogous to how window glass solidifies as it is cooled from a high temperature.

A colloidal suspension is composed of small solid particles in a liquid, like ink or paint. The key control parameter is the volume fraction ϕ: the fraction of volume occupied by the solid particles. Samples with a larger volume fraction will have a larger viscosity, and this viscosity grows quite dramatically as $\phi \to \phi_g \approx 0.58$. As the glass transition volume fraction ϕ_g is approached, the sample's behaviour parallels the glass transition of more traditional (molecular or polymer) glass-forming systems [1]. In a chunk of window glass, the atoms are arranged in an amorphous fashion; likewise, in a dollop of glassy colloidal paste, the colloidal particles are arranged in an amorphous way. Given the size of colloidal particles ($\sim$10 nm–10 μm diameter), they can be studied using a variety of techniques that are difficult or impossible to adapt to molecular glass-formers.

In the following subsections, we introduce basic concepts such as colloids, glasses and some relevant physics, before proceeding with the rest of the review.

1.2. Introduction to the glass transition

Upon slow cooling or compression, many liquids freeze—that is, the molecules constituting the liquid rearrange to form an ordered crystalline structure. In general, nucleating a crystal requires undercooling. Some materials can be substantially undercooled without crystal nucleation; alternatively, a sample can be cooled faster than nucleation can occur. In such situations, the liquid is termed *supercooled*. If the sample is sufficiently cold and cooling is adequately rapid, the material can form a glass: the liquid-like structure is retained but the microscopic dynamics all but cease. This sudden arrest is the *glass transition*, and the temperature at which it occurs is the glass transition temperature, T_g. As the liquid is cooled towards T_g, its viscosity rises smoothly and rapidly, and below T_g the sample's viscosity becomes so high that for most practical purposes it is considered a solid. The science of the glass transition is discussed in many review papers [2–10]. *Supercooled liquid* refers to a system under conditions for which it still flows, but for which the liquid is a metastable state and the thermodynamically preferred state is a crystal. The study of the glass transition then is the study of how a supercooled liquid changes as the temperature T is decreased towards T_g, and the study of glasses is the study of materials under conditions where $T < T_g$. Glasses can also be formed at constant T by increasing pressure [11, 12].

Calling a glassy material a 'solid' depends on time scales, and perhaps one's patience [13]. Window glass, a vitreous form of silicon dioxide, is of course the quintessential example of glass. It is sometimes claimed that very old windows are thicker at the bottom due to flow of glass. However, the thickness variations in antique windows are the result of a particular manufacturing method rather than the result of the glass flowing over long times [14, 15]. A more instructive example of glassy behaviour and time scales can be seen in pitch, a bituminous tar. Like window glass, pitch is unmistakably solid to the touch—if struck with a hammer, it will shatter. However, for over 80 years a funnel filled with pitch has been dripping at a rate of roughly one drop every 100 months, yielding a very approximate viscosity of 10^{11} times that of water. The so-called 'pitch drop experiment' has been housed at the University of Queensland in Brisbane, Australia since 1927 [16].

1.3. Introduction to colloids

The term *colloid* describes a wide range of multiphasic substances composed of particles (solid, liquid or gaseous) roughly 10 nm–10 μm in size dispersed in a continuous phase. Depending on the state of matter of the various phases, colloids can be divided into several categories, including, but not limited to:

- suspensions/dispersions—solid particles in a liquid (this review's main focus);
- emulsions—liquid droplets in an immiscible liquid;
- foams—gas bubbles in a liquid or solid medium;
- aerosol—liquid droplets or solid particulates in a gas.

Hence, *colloid* is equally apt to refer to a variety of systems: such as ink, paint, peanut butter, milk and blood (suspensions); Styrofoam™, shaving cream and ice cream (foams); mayonnaise and hand lotion (emulsions); hair spray and smoke (aerosols). For this range of size, colloids behave as systems of 'classical' particles where quantum mechanical effects can be largely ignored, though it is important to understand the role of quantum phenomena such as van der Waals attractions. More importantly, colloidal particles are small enough that thermal fluctuations are extremely relevant. For example, in a suspension, random collisions between solid particles and solvent molecules lead to Brownian motion, easily observed in experiments.

Aside from the everyday items mentioned previously, industrial processes such as liquid and mineral purification, oil recovery and processing, detergency and even road surfacing employ colloids to varying degrees [17]. Dense colloidal suspensions can be heated and allowed to flow while retaining some rigidity. Hence, they can be moulded, extruded and subsequently solidified to form a multitude of components. The manufacture of many types of optics, insulators, bricks and ceramics involve colloids [18].

While these examples span a wide range of useful materials, colloids also find use in laboratories as models for phases of matter. During the late 1960s and early 1970s, experiments demonstrated that structures in colloidal suspensions can be analogous to those in atomic systems [19–21], leading to extensive use of colloids over the next decade as model liquids and crystals [22–30]. In 1982, Lindsay

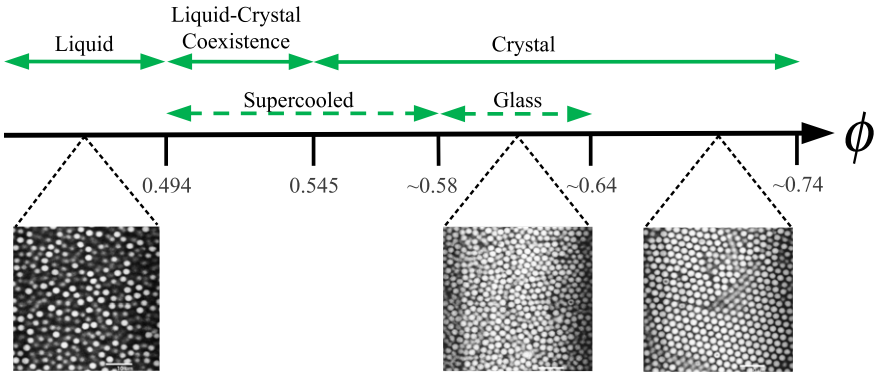

Figure 1. Top: phase diagram of monodisperse hard spheres as a function of volume fraction, ϕ. Solid arrows indicate equilibrium states, whereas dashed arrows are non-equilibrium states. Note that the existence of the glassy state requires some polydispersity (at least 8%); a more monodisperse sample will eventually crystallize [40–44]. However, polydispersity also shifts the boundaries between liquid and crystal to slightly higher values [40, 45, 46]. On the other hand, adding a slight charge to the particles shifts the phase boundaries to lower values [47, 48]. More highly charged particles shifts the phase boundaries substantially [47, 49]. Bottom: confocal micrographs of the analogous phases in a colloidal suspension with 5% polydispersity.

and Chaikin combined two different sizes of charged colloidal particles and observed a glassy phase (amorphous structure, finite rigidity) [13] in agreement with subsequent simulations [31]. Later in 1986 and 1987, experiments by Pusey and van Megen demonstrated a hard-sphere colloidal glass transition in a concentrated sample of uncharged colloids [30, 32, 33].

1.4. Basic physics: hard-sphere-like colloids

Perhaps the simplest interaction between two particles is that of *hard-spheres* [34]. If r defines the distance between two sphere centres, and σ is the sum of the two sphere radii, the hard-sphere potential is given by

$$V(r) = \begin{cases} \infty, & \text{if } r \leqslant \sigma, \\ 0, & \text{otherwise,} \end{cases} \tag{1}$$

which is to say that the only restriction placed upon the system is that particles cannot interpenetrate. Hence, all allowable configurations have identically zero potential energy. From a viewpoint of statistical mechanics, this implies that the free energy, $F = U - TS = (3/2)Nk_BT - TS = (\text{const} - S)T$, is governed entirely by entropy [35, 36], which for monodisperse systems (systems of a single-particle size) means that the only control parameter is volume fraction [1, 37–39]. Volume fraction, $\phi = NV_p/V$, is a dimensionless analogue of particle number density, where N is the number of particles in the system, V_p is the single-particle volume and V is the total system volume. (Note that the particle size controls how fast a system evolves due to diffusion, but does not control the phase behaviour; see section 1.5 for a discussion of particle size effects.)

The phase diagram for hard spheres is shown in figure 1 as a function of ϕ. Below the freezing point, $\phi_{\text{freeze}} = 0.494$, the suspension is a liquid. Forcing the system into a supercooled or glassy state requires increasing ϕ fast enough to avoid crystallization. The supercooled region persists between $0.494 \leqslant \phi < \phi_g \approx 0.58$, whereas the glassy region lies between $\phi_g < \phi < \phi_{\text{rcp}} \approx 0.64$. The existence of a glassy phase for hard-spheres requires that the sample be somewhat polydisperse, that is, the spheres must have a distribution of sizes [40–44]. The upper bound of the glassy region is the volume fraction at random close packing, ϕ_{rcp}, the maximum density of a completely random sphere packing [50–52]; the precise value of ϕ_{rcp} depends on the polydispersity [53]. Above ϕ_{rcp}, samples must have domains of crystalline structure, or, preferably from the thermodynamic point of view, the sample may be entirely crystallized. Density can be further increased up the limit of hexagonal close packing, $\phi_{\text{hcp}} = \pi/3\sqrt{2} \approx 0.74$. Hard spheres are often simulated to study the glass transition [43, 44, 54–59].

In many cases, colloidal particles can be considered to be simple hard-spheres [30, 32, 60, 61]. The first experimental demonstration of a colloidal hard-sphere glass transition was by Pusey and van Megen in the mid-1980s, who essentially replicated the hard-sphere phase diagram using colloidal samples [30, 32]; see, for example, the pictures in figure 1. The system used in these studies is particularly important for the following reasons: the interactions between particles are of a simple, well-described nature; the simplicity of the interaction allows for comparison with a wide range of systems and easy simulation with computers; they can be studied by techniques such as microscopy, light scattering and rheology—that is, a single sample can be divided and studied by an array of methods. For these reasons, along with the fact that particles are commercially available or can be synthesized readily [62–65], the same types of colloids are still widely used today.

The particles used by Pusey and van Megen were composed of poly(methyl methacryalate) (PMMA) and were sterically stabilized by the addition of a thin surface layer (≈10 nm) of poly-(12 hydroxystearic acid) (PHSA) to minimize aggregation due to van der Waals forces. It is this steric stabilization layer that allows particles to be considered as hard spheres, at least until they are forced close enough to compress the PHSA [66]. These colloids are stable in organic solvents and can be somewhat tailored for experiments, such as being dyed for use in fluorescence microscopy [64, 65, 67].

Solvent choice also allows for a greater degree of control. Miscible solvents can be mixed to closely match the density of the particles, minimizing gravitational effects that can be quite significant in studying colloidal glasses [68–70] (discussed below). Solvents can also be blended to closely match the refractive index of the particles, which both lessens van der Waals attractions and allows for use in microscopy or light scattering.

The size range and time scales that accompany colloidal particles are accessible to a variety of experimental techniques such as optical microscopy or light scattering. For example, a micrometre-sized particle in water will diffuse its diameter in about a second, which is easily observable for modern microscopes.

It is important to note that colloidal systems differ from their atomic counterparts in several ways [71, 72]. First, short time motion is diffusive in colloids, rather than ballistic. Second, hydrodynamic effects couple particle motions in complex ways [73]. Simulations suggest that these two differences are unimportant for studying the glass transition [74–80] (see also the discussion in section 2.6). A third difference is that colloidal particles are most typically spherically symmetric, and so the geometry of a molecule is usually not replicated in the colloid (see section 5 for recent exceptions). Again, for many cases of interest, this difference is immaterial when studying long-time dynamics; certainly many glass transition simulations study particles with spherically symmetric potentials. A fourth difference is that colloidal suspensions are always slightly polydisperse. This shifts the phase transitions shown in figure 1 to higher values of ϕ [40, 45, 46], and also in general frustrates crystallization [41, 43, 44, 81, 82]. While this is a distinction in comparison with simple molecular glass-formers, it is less of a distinction with simulations, which often purposefully add polydispersity to frustrate crystallization [83, 84]. Indeed, as noted in the caption of figure 1, polydispersity appears necessary for a hard-sphere glass transition; monodisperse samples always eventually crystallize [43, 44].

A final distinction is that colloidal samples are influenced by gravity. As observed in one experiment, a sample that was a colloidal glass on Earth spontaneously crystallized in microgravity [69]. Precisely matching the density of particles and solvent also potentially leads to crystallization and can have a striking influence on the ageing of a glassy colloidal sample [68, 70] (see section 4.2 for a discussion of ageing). However, the interpretation of these results is controversial. The crystallization seen may be due to differing polydispersity which strongly influences nucleation [43] and may be a confounding variable in these experiments [41, 42, 44, 82, 85]. It may also be due to heterogeneous nucleation at the walls of the sample chambers [30]. Given the robust similarities between colloidal experiments and gravity-free simulations (described in detail in section 2.6), it seems plausible that gravity is typically not a critical factor, but we note this is debatable.

Although PMMA colloids are a widely used model system, they are by no means the only colloidal system used to study the glass transition. Other non-hard-sphere systems will be discussed throughout this review, particularly in section 5.

1.5. More basic physics: diffusion and sedimentation

Two key concepts for thinking about the colloidal glass transition are diffusion and sedimentation. Diffusion sets the rate of the dynamics, and sedimentation can limit the duration of experiments.

The size of colloidal particles is such that they execute Brownian motion due to frequent, random collisions with solvent molecules. Because collisions are random in magnitude and orientation, the average particle displacement in a particular direction $\langle \Delta x \rangle$ is zero. Instead, motion is quantified by the mean square displacement (MSD),

$$\langle \Delta x^2 \rangle = \langle [x(t + \Delta t) - x(t)]^2 \rangle = 2D\Delta t. \tag{2}$$

The angle brackets $\langle\rangle$ indicate an average over all particles and all initial times t for a particular lag time Δt, and D is the diffusion coefficient. In three dimensions, (2) becomes

$$\langle \Delta r^2 \rangle = 6D\Delta t. \tag{3}$$

For a single particle of radius a immersed in a solvent of viscosity η, the diffusion coefficient D is given by the Stokes–Einstein–Sutherland equation,

$$D = \frac{k_B T}{6\pi \eta a}, \tag{4}$$

where k_B is Boltzmann's constant and T is the system temperature [86, 87]. This equation shows that T, η and a do not play a direct role in the colloidal glass transition; they only influence D, which in turn sets a time scale for particle motion. This time scale is the diffusive (or Brownian) time,

$$\tau_D = \frac{a^2}{6D} = \frac{\pi \eta a^3}{k_B T}, \tag{5}$$

which is the average time needed for a particle to diffuse its own radius (using $\langle \Delta r^2 \rangle = a^2$ in (3)).

For purely diffusive motion, such as in a dilute suspension, the MSD scales with Δt. Thus, on a log–log plot of $\langle \Delta r^2 \rangle$ versus Δt, one expects a straight line with a slope of unity. The MSD for a colloidal sample at $\phi = 0.52$ is shown in figure 2(a). At the smallest Δt, the MSD shows diffusive behaviour, indicated by the dashed lines. Note that the diffusion constant obtained from this short time-scale motion, D_S, differs from that of (4) for $\phi > 0$ due to hydrodynamic interactions between the particles [88–92]. D_S drops to approximately 50% of the value from (4) by around $\phi \approx 0.3$.

As the lag time increases, a plateau develops in the data of figure 2(a) which is indicative of particles being trapped in cages formed by their neighbours. At these time scales, particles are localized and large cumulative motions are suppressed [2, 93–98]. At sufficiently long Δt, particle rearrangements do occur, and so the MSD again increases, eventually recovering diffusive behaviour. Figure 2(b) shows the MSDs measured with light scattering for samples at several volume fractions (see section 2.4 for a discussion of light scattering). As ϕ increases from left to right, one observes a lengthening of the plateau and thus increasingly slowed dynamics. The plateau heights in figure 2(a) are at $\langle \Delta x^2 \rangle / a^2 \sim 5 \times 10^{-3}$, whereas in ($b$) they are at $\langle \Delta r^2 \rangle / a^2 \sim 10^{-1}$. For panel ($a$) the data could be multiplied

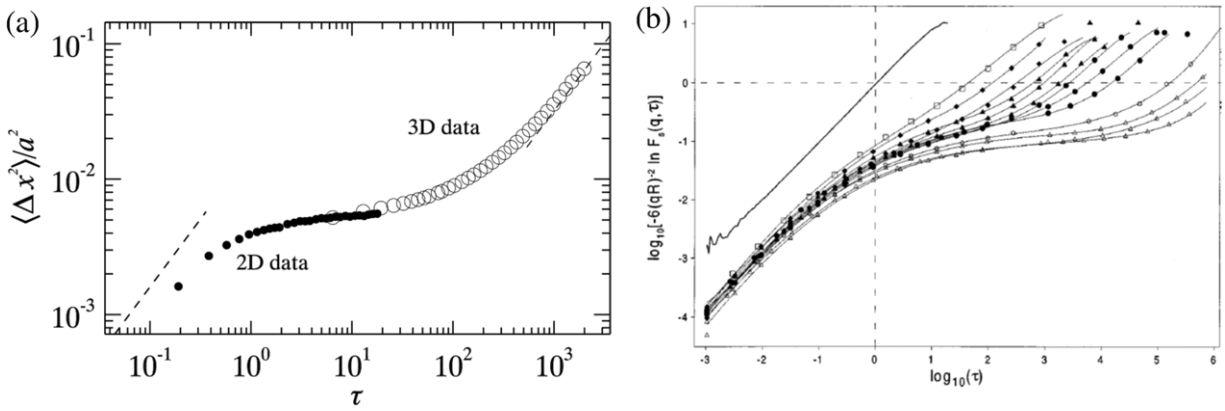

Figure 2. (*a*) An example MSD from a sample with $\phi = 0.52$, observed with confocal microscopy. Particles have radius $a = 1.18\,\mu$m. Data are from [99]. The horizontal axis has been normalized by the diffusive time ($\tau_D = 2.79$ s for these particles) and the vertical axis has been normalized by a^2. The two-dimensional (2D) data (solid circles) are collected at a fixed depth within the 3D sample, while 3D data (open circles) are collected over a fixed sample volume. The 2D data can be acquired more rapidly and probe shorter time scales, which is why the two data sets extend over different ranges in Δt. The graph shows only the x-component of the MSD, but the y- and z-components are similar. The dashed lines indicate a slope of 1. (*b*) MSDs measured via light scattering. Time scales are normalized by the diffusive time ($\tau_D = 0.0215$ s) and measured at $qR = 1.3$ using the particle radius $R = 200$ nm (here q is used instead of k for the wave vector). The horizontal dashed line corresponds to the particle size a^2. Volume fraction increases from left to right: $\phi \approx 0$ (solid line), 0.466 (squares), 0.502, 0.519 (closed diamonds), 0.534, 0.538, 0.543, 0.548 (closed triangles), 0.553, 0.558 (closed circles), 0.566 (stars), 0.573, 0.578, 0.583 (open triangles). Figure (*b*) is reprinted with permission from [100], copyright 1998 by the American Physical Society.

by 3 to convert from $\langle x^2 \rangle$ to $\langle r^2 \rangle$, giving a plateau height of $\sim 1.5 \times 10^{-2}$, still smaller than the data in panel (*b*). The difference is very likely due to the different colloidal particles used: those in (*a*) are slightly charged [99], whereas those in (*b*) are more nearly ideal hard spheres [100]. The additional repulsion between charged particles would presumably reduce the amplitude of motion within the particle cages, thus reducing the MSD plateau height. The upturns in the MSD for figure 2(*a*) ($\phi = 0.52$) and the solid diamond symbols in figure 2(*b*) ($\phi = 0.519$) are roughly at $\tau \sim 10^2$; differences may be due to the differing particle interactions, but are equally likely to be due to differences in ϕ, given the uncertainty of each experiment's volume fraction measurement [66].

The overall shapes of the MSDs in figure 2 are typical of dense suspensions. In these cases, one often characterizes the system in terms of a long-time diffusion constant, defined as

$$D_L \equiv \lim_{t \to \infty} \frac{\langle \Delta r^2 \rangle}{6 \Delta t}. \tag{6}$$

This describes the motions within a system at times after the plateau in the MSD, as shown at large lag times in figure 2.

If the particle size is doubled in a colloidal sample while keeping the volume fraction ϕ constant, then the motion slows by a factor of 2 on an absolute scale (from (3) and (4)) and a factor of 8 relative to the particle size (from (5)). However, the overall appearance of the dynamics (liquid-like or glassy) remains the same: more specifically, the behaviour of $\langle \Delta r^2 \rangle / a^2$ as a function of $\Delta t / \tau_D$ is unchanged. This suggests a useful experimental technique: to effectively explore long-time dynamics, one might use smaller colloidal particles which diffuse faster and reach the long-time behaviour on relatively short experimental time scales. In contrast, video microscopy techniques (section 2.1) work better with slower moving particles, so one typically uses larger particles in such experiments.

The other important consideration for colloidal glass experiments is sedimentation. It is tricky to match the density of the solvent to the density of the colloidal particles, and so over time particles sink to the bottom of a sample chamber (or float to the top). This changes the local volume fraction, the key control parameter, and so sedimentation is important to understand for experiments.

The length scale over which gravity is important is set by balancing the gravitational potential energy $\Delta \rho V_p g z$ with the thermal energy $k_B T$, where $\Delta \rho$ is the density difference between the particle and the solvent, $V_p = \frac{4}{3} \pi a^3$ is the volume of the particle, g is the acceleration of gravity and z is a height. Solving this for z gives the scale height

$$z_0 = \frac{3}{4\pi} \frac{k_B T}{\Delta \rho a^3 g}. \tag{7}$$

In equilibrium, ϕ varies over distances $\sim z_0$. In particular, one expects to find $\phi(z) \approx \phi_0 \exp(-z/z_0)$ for $\phi \ll \phi_g$. If a sample chamber has a height much less than z_0, then sedimentation can probably be ignored. This is achieved using thin sample chambers, $\sim 200\,\mu$m thick typically. Alternatively, one can use small particles; as (7) shows, $z_0 \sim a^{-3}$. More careful matching of the density of the solvent can minimize $\Delta \rho$; here, the chief problem is that solvent and particle densities depend on T, so $\Delta \rho$ is only minimized for one particular temperature.

If a colloidal sample is stirred, the initial volume fraction can be fairly homogeneous, and some time is needed to reach the equilibrium volume fraction gradient. This amount of time can be estimated from the sedimentation velocity. The Stokes drag force on a sphere moving with velocity v is

$$F_{drag} = 6\pi \eta a v. \tag{8}$$

The gravitational force acting on a colloidal particle is given by

$$F_{grav} = \tfrac{4}{3} \pi a^3 \Delta \rho g. \tag{9}$$

Balancing these two gives the sedimentation velocity as

$$v_{\text{sed}} = \frac{2}{9}\frac{\Delta\rho g a^2}{\eta}. \quad (10)$$

In practice, the sedimentation velocity is much slower for high-volume fraction samples due to the backflow of the solvent through the sedimenting particles [101–103]. However, v_{sed} can be used to find a crude estimate for relevant time scales: the volume fraction gradient should be established in time scales of order $z_0/v_{\text{sed}} \sim a^{-5}\Delta\rho^{-2}$, for example. Measuring v_{sed} in a centrifuge (increasing g) can be used to estimate $\Delta\rho$, again being mindful of the temperature dependence of $\Delta\rho$.

Considerations of diffusion and sedimentation lead to the conclusion that, all else being equal, smaller particles are preferred. However, other experimental considerations often dictate that larger particles be used. Where appropriate, this will be commented on in section 2 which deals with experimental techniques. Another possibility is to use colloids that are much better density matched, and microgel particles are powerful in this regard [104, 105]. These particles are crosslinked polymers used in a good solvent, where the particle is swollen and permeated with solvent, and thus the density matching is much less an issue.

1.6. Overview of the rest of review

The goal of this review is to familiarize the reader with current knowledge of properties of colloidal suspensions in the glassy state ($\phi_g \lesssim \phi \lesssim \phi_{rcp}$) or very near to it ($\phi \to \phi_g$). In particular, we focus mostly on experimental results; for a more theoretical approach, the interested reader should consider other recently published review articles [1, 9, 10, 72, 106]. The majority of our attention will be given to hard-sphere-like colloids, as many experimental and simulational results concern these systems. We will, however, compare and contrast these observations with other colloidal glasses, as well as with atomic and molecular glasses when appropriate, and describe some theoretical attempts to understand the nature of the glass transition.

Section 2 reviews experimental techniques within the field. It is by no means a complete review of any specific technique, and so references will be given for further reading. Section 3 discusses what is known about the glass transition, that is, $\phi \to \phi_g$, and section 4 discusses properties of glasses, samples with $\phi > \phi_g$. Section 5 discusses other soft glassy materials, and section 6 is a brief conclusion. Specific discussions of the strengths and weaknesses of colloids as models for glasses are found in section 1.4 (differences between colloids and molecules), section 2.6 (colloids as models compared with simulations as models) and section 6 (focus on strengths of colloids as a model system and discussion of the value of ϕ_g).

2. Important techniques

2.1. Video microscopy

Microscopy has been used to study colloidal suspensions since the work of Brown and his contemporaries, who reported on the thermal motion of colloidal particles; a good historical account of these observations is [107]. In modern times, the availability, commonality and relative ease-of-use of optical microscopes and video cameras have made video microscopy a popular technique. Whether used in a biology, biochemistry, or physics setting, the mode of operation is the same: a microscope is used to visualize a system; a camera is coupled to the microscope and is used to capture images; and, some type of recording media stores the images for later analysis [108]. Probably the most familiar form of microscopy is brightfield microscopy. Brightfield microscopy relies on scattering or absorption of light by the sample to produce image contrast. Scattering occurs when small differences in the sample's refractive index cause light to deviate from its initial path, leading to a brightened or darkened region in an image. The amount of absorption depends on the material properties of the sample, but image contrast can often be enhanced by the addition of dyes. Modifications of brightfield microscopy include darkfield microscopy, phase contrast microscopy and differential interference contrast microscopy—all of which are effective at improving image contrast when the variations in refractive index are small, such as the case of a living cell (filled mostly with water) in a watery medium [108, 109].

Brightfield microscopy is particularly easy when the sample is quasi-two-dimensional (quasi-2D). For example, quasi-2D colloidal glasses have been studied confined between parallel plates [110, 111] or at an interface [112, 113]. In such experiments, particles always remain in focus and microscopy is quite easy.

A second important type of microscopy is fluorescence microscopy. In this case, the illuminating light is high energy (short wavelength), which excites a dye and causes the emission of longer wavelength light. The advantage of fluorescence microscopy over brightfield is that specific constituents of a sample can be dyed, such as particles in a colloidal suspension, and thus selectively observed [108]. However, the main drawback of using dyes in a sample is that they can lose their ability to fluoresce with increased exposure to light and oxygen—an effect called photobleaching. This means that, over the course of an experiment, the portion of the sample which is being observed will become dimmer. When studying colloidal glasses, the effect of photobleaching is often minor; the time between successive images can be safely set to be on the order of tens of seconds because the dynamics are slow, minimizing the system's exposure to light.

In some cases, the presence of a dye can modify the interactions within a system. For example, in the case of PMMA particles some dyes can leave a small residual electric charge on the particle, causing them to behave as slightly soft spheres rather than hard ones (though this can be countered by adding salts to the solvent [114–116]). Additionally, dyes can decay over time and, over long times, can even diffuse out of the particles and into the solvent, making imaging difficult.

A good general discussion of video microscopy is [117]. Applications of video microscopy to colloidal suspensions are reviewed in [29, 108, 118].

2.2. Confocal microscopy

Conventional optical microscopes are not well suited for 3D microscopy. In order to see deep within a sample,

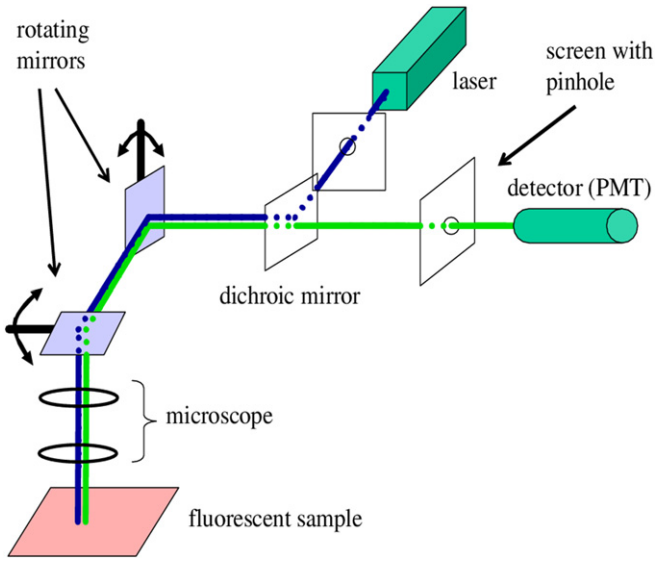

Figure 3. Schematic of a confocal microscope. Rotating mirrors scan the incoming laser light over the region of interest in the sample. The emitted light follows the reverse optical path until arriving at the dichroic mirror, where it passes through the pinhole and into the detector. A dichroic mirror reflects light below a certain wavelength and transmits light above it. Reproduced with permission from [119].

it is necessary to minimize the scattering of light by closely matching the refractive indices of the particles and solvent. Without scattering, conventional optical microscopy is difficult. Fluorescence microscopy overcomes this using the contrast between dyed and undyed portions of the sample to produce an image. This works well for dilute samples, but is poorly suited for dense systems such as colloidal glasses. Because the sample is nearly transparent, objects outside of the focal plane are fluoresced, and stray background light passes readily through the optics and can severely muddle an image: it is hard to distinguish bright particles on a bright background. Confocal microscopes use fluorescence as well, but overcome this limitation with special optics (described below) and are much better suited for studying dense colloidal systems.

The functioning of a confocal microscope hinges on two principles: illumination of a small sample volume ($\leqslant 10^{-15} L$) and rejection of out-of-focus light [119]. A schematic of a confocal microscope is shown in figure 3. Laser light, shown in black (blue online), passes through a dichroic (dichromatic) mirror and onto rotating mirrors that scan the light in the horizontal planes. The light then passes through the microscope optics and excites the fluorescent sample. The emitted light, shown in dark grey (green online), follows the reverse optical path back to the dichroic mirror, where it is reflected onto a screen with a pinhole. The pinhole is placed in the *conjugate focal* plane of the sample (hence the term *confocal*), rejecting the vast majority of out-of-focus light and limiting the depth of field [118]. The remaining in-focus light is finally collected by a detector, such as a photomultiplier tube.

Confocal microscopy allows for direct imaging of a sample in two or three dimensions. In two dimensions, an image is constructed by scanning individual points (point scanning microscopes) or lines of points (line scanning

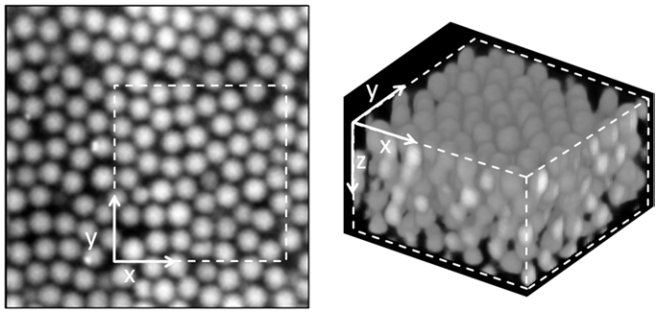

Figure 4. Left: confocal micrograph of a monodisperse colloidal system at volume fraction $\phi \approx 0.63$. The particles have diameter $2a = 2.1\,\mu$m and the image is taken at the coverslip, where the particles layer against the wall. Right: 3D reconstruction of the boxed region on the left. Here, the image dimensions are $15 \times 15 \times 10\,\mu\text{m}^3$.

microscopes) over a sample. The highest rates of scanning are achieved with use of an acousto-optical device (AOD), in which one of the mirrors in figure 3 is replaced with a crystal that acts as a diffraction grating whose grating spacing can be tuned with high-frequency mechanical vibrations [120, 121]. Another option is to use a Nipkow disc, which scans many points simultaneously [122]; these systems achieve high speeds, although more illuminated points slightly increases the background fluorescence detected at any given point.

To obtain 3D images, such as shown in figure 4, the 2D scanning procedure is quickly repeated while the focal plane is advanced through different depths in the sample. In the fastest modern confocals, 2D images can be collected at rates $\approx$100 frames s^{-1}, and depending on the scanning depth, 3D images can be collected in around 1 s. The specific details (times, pixels) vary from system to system, although it is worth noting that dynamics in dense colloidal systems are quite slow near the glass transition, so even slower confocal microscopes can still obtain adequate images from glassy samples.

The earliest observations of colloids using confocal microscopy were done by Yoshida *et al* in 1991 [123] and van Blaaderen *et al* in 1992 [124]. Yoshida *et al* examined colloidal crystallization near walls, and later studied colloidal gels [125]. van Blaaderen *et al* demonstrated the utility of fluorescent core–shell particles and confocal microscopy. Core–shell particles are ones with small fluorescent cores and non-fluorescent shells, so that their centres are bright dots that are well separated in the image from other particle centres even at high-volume fractions. The early work of van Blaaderen *et al* nicely demonstrated the power of confocal microscopy with important proof-of-principle measurements, and hinted at applications using particle tracking [124, 126]. In 1995, van Blaaderen and Wiltzius applied particle identification software to locate the positions of several thousand particles in 3D confocal images to investigate the structure of a colloidal glass [127], sparking much subsequent work [128, 129]. The key 1995 finding was that the structure of a colloidal glass was quite similar to the glassy structure seen in simulations.

More details of applying confocal microscopy to colloidal samples can be found in [119, 130], and a good starting point to learn about confocal microscopy is [131].

2.3. Particle tracking

Particle tracking incorporates various image processing and computational techniques to identify the centroid positions of particles in a given image [118, 132]. Images can be 2D, as in brightfield or fluorescence microscopy, or 3D, as in confocal microscopy. Repeating the procedures for consecutive images yields a list of coordinates at subsequent times. The coordinates can be used immediately to obtain structural information about a sample, or if dynamic information is desired, the coordinates can be linked together in time to form individual particle trajectories.

In general, the larger a particle is in an image, and the more it contrasts with the background, the more accurate the particle tracking. As mentioned in section 1.5, however, larger particles move slower and are more prone to sedimentation. For many experiments, particle centres can be located with a resolution of approximately 20 nm in the focal plane, while the out-of-plane resolution is typically no better than 50 nm. Recently, algorithms have been developed that push spatial resolution to ≈5 nm [133, 134].

In dilute samples, accurately identifying particles is relatively easy because bright and well-separated particles contrast well with the dark background. In dense samples like colloidal glasses, there are many bright particles in an image and so contrast is usually poorer. Additionally, optical effects such as diffraction can make it difficult to distinguish individual particles when they are very close together. These effects are important to understand and correct, especially when particle motions are very small [135, 136]. To illustrate, in a sample of 2.4 μm diameter PMMA spheres at $\phi = 0.52$, Weeks and Weitz observed the majority of particles to move less than 0.2 μm over 600 s [137]. The influence of diffraction can be weakened by increasing the optical resolution using fancier lenses [117], using confocal microscopy (see section 2.2), or with computational techniques [134, 135]. Hence, with some care as far as optics are concerned, and some fine tuning of particle-tracking parameters, it is often straightforward to study dilute and dense systems with the same techniques.

Combined with video microscopy, particle tracking offers a powerful method to probe the local properties of a sample, which is especially important for understanding structurally or dynamically heterogeneous systems like colloidal glasses. With this technique, one can discuss behaviours of individual particles up to a collection of several thousand. This degree of resolution is not available with light scattering (see section 2.4) or conventional rheology (see section 2.5) where quantities are averaged over thousands to millions of particles. However, such a small statistical sampling can make it difficult to draw conclusions about a system's bulk properties without collecting an overwhelming amount of data.

The main starting point for particle tracking is the original paper by Crocker and Grier [132], and the software described in the paper is available for download on the web [138]. Samples that are flowing or being sheared can also be tracked using pre-treatment of the data; see [139] for details. For a comprehensive assessment of particle tracking, see [134].

2.4. Static and dynamic light scattering

Light scattering is a powerful technique for probing the average structure and dynamics of a sample. A laser is aimed at a sample, and the light scattered from the sample at a given angle is detected.

Photons scattered from different portions of the sample interfere with each other, and how this interference (constructive or destructive) depends on angle provides information about the structure of the sample. In particular, this information leads to the static structure factor $S(k)$, the Fourier transform of the particle positions. This is static light scattering (SLS). The scattering wave vector k is given by $k = [4\pi n/\lambda]\sin(\theta/2)$, where λ is the laser wavelength, n is the index of refraction of the sample medium and θ is the angle between the incident light and detected light [119, 140, 141].

In dynamic light scattering (DLS), the light intensity, $I(t)$, at a fixed angle is monitored as a function of time. The light intensity fluctuates as portions of the sample rearrange, changing the interference pattern of scattered light. In particular, one monitors how the intensity autocorrelation function,

$$g_2(\Delta t) = \frac{\langle I(t+\Delta t)I(t)\rangle_t}{\langle I(t)\rangle^2}, \tag{11}$$

changes as a function of lag time Δt. At $\Delta t = 0$, $g_2(\Delta t)$ is at a maximum, and decays from this value as the sample evolves. Scattering functions, such as the self-intermediate scattering function shown in figure 5, are related to $g_2(\Delta t)$ and are used to quantify dynamics. By measuring the rate of decay, one measures how particles move and can extract information similar to the diffusion coefficient. Probing the dynamics at different k values allows one to determine information about either local or collective particle motion within the sample; most typically, k is chosen to coincide with the peak of the structure factor $S(k)$, which yields information about collective motions. Alternatively, tracer systems can be prepared and single-particle motion probed [100, 142], or else the behaviour at $k \to \infty$ can be examined which also relates to self-diffusion [89]. For example, the MSDs in figure 2(*b*) are calculated from the DLS data in figure 5. The autocorrelation function is often calculated over time scales down to 10^{-6} s, allowing a large range of time scales to be measured, as shown in figure 5. For more details about both SLS and DLS, see [140, 141].

The main strength of light scattering is that light is scattered from a significant volume within the sample, typically containing millions of particles. The measurement is a very good average of information from all of the particles, whether it be structural information (SLS) or dynamic information (DLS). For DLS, given that the measurement is sensitive to motions corresponding to fractions of λ, accurate MSDs are straightforward to obtain. However, because of the ensemble-averaging properties, local information is harder to obtain. For example, while calculating the MSD is easy, knowing how individual particle motions are correlated in space is more difficult. A secondary strength of light scattering is that typically particles smaller than those in microscopy experiments can be used, for example 300 nm radius [54] in one early experiment. These smaller particles are much

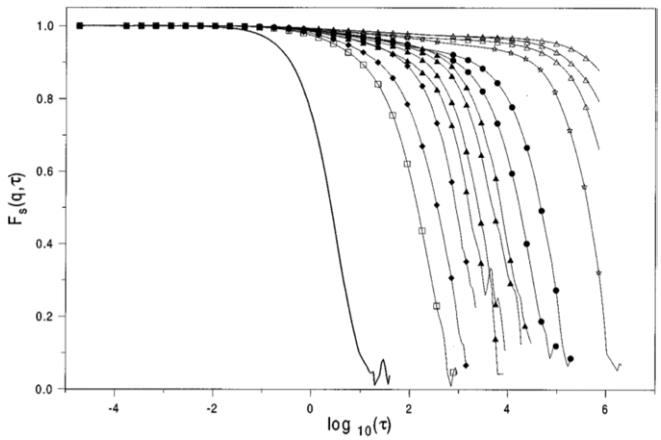

Figure 5. Self-intermediate scattering functions, $F_s(k, \tau)$, as a function of the dimensionless time $\tau = \Delta t/\tau_D$ with $\tau_D = 0.0215$ s, and measured with wave vector $kR = 1.3$. Data and symbols are the same as in figure 2(*b*). Note that an increase in ϕ corresponds to an increase in decay time. Reprinted with permission from [100], copyright 1998 by the American Physical Society.

less affected by sedimentation (see section 1.5). Additionally, smaller particles diffuse faster, allowing their motion to be probed over a larger range of time scales.

In 2001, Williams and van Megen devised a clever method to examine binary samples (mixtures of two particle sizes) with SLS and DLS [143]. Their size ratio was $a_{small}/a_{large} = 0.6$. They slightly modified the synthesis method for the two particle types so that they had distinct indices of refraction. By tuning the temperature of the solvent, they could closely match the index of one or the other particle type, and obtain information about each particle species independently. These experiments nicely demonstrated that at a given volume fraction, mixtures of two sizes are more liquid-like than a monodisperse sample [143], in agreement with viscosity measurements [144, 145]. This is because binary samples can be packed to higher volume fractions than monodisperse samples, so at a given volume fraction, a binary sample has more free volume than a monodisperse sample. A subsequent experiment suggested that the small particles can 'lubricate' the motion of the large particles (size ratio $a_{small}/a_{large} = 0.48$) [146]. However, theory and simulations indicate that the opposite is true for size ratios $a_{small}/a_{large} > 0.8$ [58, 147, 148]: for such size ratios, increasing the fraction of small particles can increase the glassiness of the sample. For small size ratios $a_{small}/a_{large} \leqslant 0.1$, the depletion force becomes relevant, where the small particles effectively push together the large particles. This can lead to both more and less glassiness, depending on the conditions [149], and is further discussed in section 5.1. Binary samples in general are of interest for understanding multi-component molecular glasses, and the technique of Williams and van Megen demonstrates how light scattering can be used to study such multi-component systems [143].

In very dense colloidal suspensions, such as those near a glass transition, additional experimental issues arise. One problem is that in a glassy sample, particles do not rearrange significantly, so it is difficult to obtain a proper time-average from the sample. Several techniques have been developed to deal with this situation and are reviewed in [150–152].

A second problem is that light is often scattered from more than one particle before being detected. Again, several techniques have been developed for cases when the light scattered a few times before detection, some of which are reviewed in [152, 153]. One common technique is diffusive wave spectroscopy (DWS) [154–158] which works when light scatters many times before detection. Here, the light is assumed to be scattered so many times that each photon can be thought to diffuse randomly through the sample before exiting and being detected. Diffusion is straightforward to describe mathematically so, for a given experimental geometry, it is possible to calculate the average number of times a photon has been scattered (and therefore the number of particles from which it scattered). Again, the intensity of light is monitored and its autocorrelation calculated, but now, each particle needs only move a very small fraction of a wavelength before the sum of these motions results in significant decorrelation of the intensity. DWS is thus useful for multiply scattering samples with small motions. Colloidal glasses were studied soon after the development of DWS [157], an early result being that the MSD of densely packed particles is nonlinear in time (as shown in figure 2, for example).

DWS is reviewed in [159]. A useful review paper which briefly discusses differences between DWS and DLS is [160]. Ultra-small-angle neutron and x-ray scattering as applied to colloidal glasses is reviewed in [161]; these techniques can probe structure on length scales of ∼1–10 μm. A recently published book on glasses and dynamical heterogeneity (see section 3.3) contains a chapter by Cipelletti and Weeks which focuses on colloidal glasses [162]. This chapter discusses many details of light scattering. A review paper by Sciortino and Tartaglia compares experimental data with theoretical predictions, with a focus on light scattering data [1].

2.5. *Rheology*

Rheology is the study of how materials flow and deform. A rheological measurement quantifies how solid- or fluid-like a substance is in response to a specific stress [18]; that is, the goal of rheology is to measure elastic and viscous properties of a system. To make such a measurement, one needs a *rheometer*, a device capable of either creating a constant or oscillatory stress and measuring the resulting rate of deformation, or measuring the stress required to deform a material at a constant rate of strain.

An elementary rheometer is illustrated in figure 6. The device consists of two horizontal plates separated by a distance h, where the top plate is mobile and the bottom plate is fixed. On the left of figure 6, an ideal Hookean (elastic) solid is placed inside and the top plate is displaced by a distance Δx. The stress σ (≡ force/area) needed to do this is given by the relation

$$\sigma = G\frac{\Delta x}{h} = G\gamma. \tag{12}$$

This equation defines the *shear modulus* G, where $\gamma = \Delta x/h$ is the strain.

On the right side of figure 6, the rheometer is filled with a simple fluid, such as water, and the top plate is displaced at a

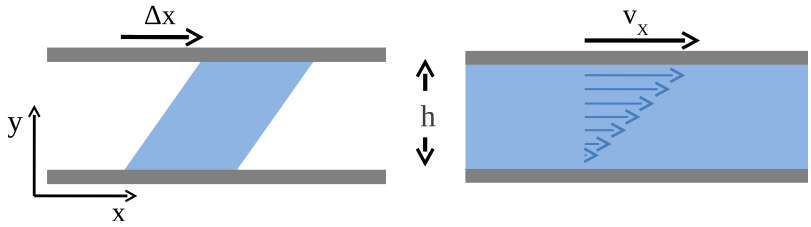

Figure 6. Schematic of a simple rheometer. Left: the top of an ideal solid is displaced Δx, leading to a strain of $\gamma = \Delta x/h$. Right: a Newtonian fluid is sheared at a rate of $\dot{\gamma} = v_x/h$.

constant velocity v_x. As the top plate moves, it drags the fluid underneath in accordance with the no-slip boundary condition of fluid mechanics. For the same reason, the fluid immediately above the fixed bottom plate is motionless. This creates a steadily decreasing velocity profile (indicated by the arrows). The shear stress needed to maintain the constant velocity of the top plate is given by

$$\sigma = \eta \frac{\partial v_x}{\partial y} = \eta \frac{v_x}{h} = \eta \dot{\gamma}. \tag{13}$$

The above equation defines the *shear viscosity* of a fluid, $\eta = \sigma/\dot{\gamma}$, where $\dot{\gamma}$ is the shear rate. Fluids that adhere to this relation are called *Newtonian fluids*.

More generally, many materials are termed *viscoelastic*: they have both a viscous and elastic nature [73, 163–167]. Viscoelasticity can be studied by applying a low amplitude sinusoidally varying strain of the form $\gamma = \gamma_0 \sin(\omega t)$. As noted above, the elastic stress is proportional to this strain and thus depends on $\sin(\omega t)$, while the viscous stress is proportional to the strain rate and thus depends on $\cos(\omega t)$. For a viscoelastic material one would measure

$$\sigma(t) = \gamma_0 \left[G'(\omega) \sin(\omega t) + G''(\omega) \cos(\omega t) \right], \tag{14}$$

where the two moduli are the *storage modulus* $G'(\omega)$, and the *loss modulus* $G''(\omega)$. These two moduli in general depend on the frequency ω. G' describes the ability of the material to store elastic energy, while G'' characterizes energy dissipation. Analogous to a dampened spring, the elastic portion oscillates in phase with the stress, whereas the viscous portion is out of phase by a factor of $\pi/2$.

It is worth noting that colloidal suspensions are viscoelastic, and so their rheological properties depend on the measurement frequency, ω, as shown in figure 7 [163]. Viscoelastic behaviour has been explored both experimentally and theoretically [163, 168]. In figure 7, it can be seen that both G' and G'' rise rapidly near the glass transition over a large range of of ω.

For colloids at the glass transition, the elastic modulus $G'(\omega)$ is larger than the loss modulus $G''(\omega)$ for a wide range of frequencies, and in particular as $\omega \to 0$. This latter condition corresponds to solid-like behaviour for a quiescent sample. Related to this is the idea of a yield stress, that a solid-like sample requires a finite stress be applied in order for the sample to flow (flow being defined as $\dot{\gamma} > 0$ for a given applied stress) [166].

There exist techniques to measure viscosity and elasticity from video microscopy and particle tracking, and

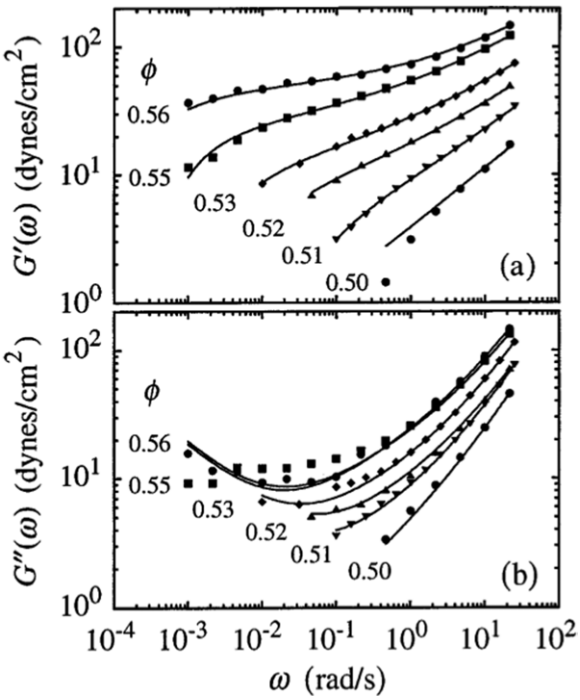

Figure 7. (*a*) Storage modulus and (*b*) loss modulus as a function of frequency for colloidal suspensions at different volume fractions. The solid lines are fits to a model based on mode-coupling theory (MCT). Reprinted with permission from [163], copyright 1995 by the American Physical Society.

light scattering; these techniques are collectively termed *microrheology* [169–173]. It is important to note that microrheology measurements represent local, microscopic properties, whereas rheological measurements involve macroscopic, bulk samples. Applying microrheology methods to dense suspensions requires care in the interpretation [174–184]. Of historical note, the first experiment to use microrheology was by Mason and Weitz in 1995, and this experiment used DWS (section 2.4) to probe colloidal glasses as a test case.

Good reviews about the rheology of colloidal suspensions include [185–189]. More general information about rheology can be found in [18, 190–192]. See also the discussion of sheared samples in section 4.3 of this review.

2.6. Simulations

As discussed above, colloidal glasses are often considered as model hard-sphere glasses, and complement simulations of

hard spheres. Likewise, simulations of hard spheres give quite useful insight to colloidal glasses, and in many cases have guided experiments.

It is difficult to simulate a large number of colloidal particles at high-volume fractions taking into account hydrodynamic interactions and interaction potentials; often approximations are desirable or necessary [193]. For that matter, colloidal glasses are themselves only approximate models of molecular glassy materials, so to the extent that colloidal glasses may provide insight into the general glass transition, one hopes that the details are not crucial and that approximations are acceptable. Fortunately, this seems to be the case. First, the microscopic dynamics seem unimportant. Simulations with Brownian dynamics (appropriate for colloids) or Newtonian dynamics (appropriate for simple hard-sphere systems without a solvent) result in similar long-time-scale dynamics [74–80]. Second, the interaction potential seems unimportant. Observations such as dynamical heterogeneities are similar in Lennard-Jones simulations [194–197], hard-sphere simulations [56, 198] and soft sphere simulations [199–202]; see section 3.3. The accumulation of evidence suggests that the specific details of colloidal interactions are not crucial for understanding glassy behaviour. The limitations of the colloidal samples as models (Brownian dynamics with hydrodynamic interactions) may also not be crucial problems for comparing colloidal glasses with molecular glasses. Third, even the dimensionality may be fairly unimportant. Simulations see similar slowing of dynamics in two dimensions and three dimensions, as well as similar particle motions [198, 203, 204]. Likewise, colloidal experiments see similar slowing and similar qualitative features in two dimensions [110, 112] and three dimensions [128, 129, 205]. One caveat is that preventing ordering is more important in lower dimensions and so binary or polydisperse samples must be used to study glass transitions in two dimensions. However, this also suggests the possibility of better understanding the role of crystallization and frustration by considering higher dimensions; see [206–208] which discuss intriguing results from 4D simulations.

Another consideration for comparing simulations and experiments are finite size effects. In a simulation, often periodic boundary conditions are used. The key assumption, then, is that the box size should be at least twice as big as any structural length scales or dynamical length scales present [8]. Of course, it is possible some of these length scales may be longer than expected—for example, one simulation found evidence for a structural length scale that was three times as large as the more obvious dynamical length scale [209]. Two simple options exist. First, one can conduct simulations for a range of box sizes, and verify that the physics one observes is independent of box size or perhaps scales in some clear way. Second, one can exploit the size dependence to learn something about the sample [210]; see the discussion in section 3.4.

In experiments, finite size effects also can cause problems. In a typical microscopy experiment, 2D images can contain a few hundred particles, or 3D confocal microscopy images can contain a few thousand particles. While the sample chamber may well be much bigger, this still limits the size of dynamical length scales that can be studied; see, for example, the discussion of finite size effects in [129]. Also, samples are often imaged through a glass coverslip, and care must be taken to take the data away from the boundaries; the presence of boundaries introduces layering [57, 211–214] and likely changes the dynamics as well [57, 215]. However, microscopy imaging is difficult deep within a sample; here light scattering has an advantage.

Given the similarities between a variety of simulations and the colloidal glass transition, this review paper will not completely survey the literature of simulational studies of the colloidal glass transition because in reality, simulations can be quite relevant for the colloidal glass transition without specifically being simulations of colloids, and this review paper cannot effectively survey all of the simulations of the glass transition. Instead, in subsequent sections of this review, as we describe features of the colloidal glass transition we will discuss the relevant simulation results.

However, some intriguing advantages of simulations are certainly worth noting here. Widmer-Cooper *et al* demonstrated advantages of the 'iso-configurational ensemble,' where they repeated simulation runs with identical starting positions for particles, but with randomized velocities; this is certainly something well suited to simulation [203, 216]. Their results are described more comprehensively in section 3.3, but briefly, their technique demonstrated that certain regions have a higher propensity for particle motion. Another interesting simulation by Santen and Krauth used non-physical Monte Carlo moves to probe 'equilibrium'-like sample properties for glassy samples [217]. They found that thermodynamic properties were continuous across the transition, evidence that the glass transition is not a thermodynamic transition. The 4D simulations mentioned above led to interesting results as crystallization is much harder in four dimensions, and so even a monodisperse system can have glassy behaviour [206–208]. These three examples—all using hard particles—give a sense of the variety of ways that simulations can give unique insight into the colloidal glass transition.

Several textbooks exist which discuss simulation techniques; a good starting point is [218]. Reviews of simulations of the glass transition include [8, 219].

A textbook introducing a large variety of methods for studying soft materials is [108]. Many of the techniques discussed above are described in more detail, including microscopy, simulation methods and rheology.

3. Features of systems approaching the glass transition

3.1. Growth of viscosity and relaxation times

A liquid's viscosity increases upon cooling. If cooling continues into the supercooled regime, the viscosity continues to grow, and at the glass transition is about 10^{13} poise [3]. (For comparison, the viscosity of water at room temperature is 0.01 P, glycerol is 15 P and honey is 100 P [220].) Analogously, increasing the volume fraction in a colloidal suspension, shown in figure 8, causes an increase in viscosity. As can be seen, the

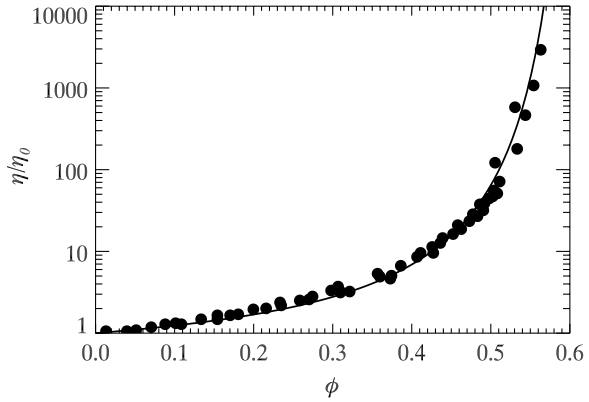

Figure 8. Scaled low shear viscosities at different ϕ for various colloidal suspensions of nearly monodisperse hard spheres. The low shear viscosities (η) are normalized by the viscosity of the pure solvent (η_0). The fit line is to equation (15) with $C = 1$, $\phi_m = 0.638$, $D = 1.15$. Data taken from [221, 225–227].

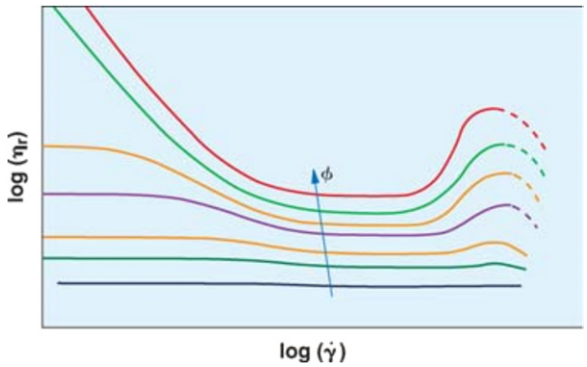

Figure 9. Schematic of shear thinning and shear thickening for colloidal suspensions at various volume fractions. Reprinted with permission from [187].

maximal change in viscosity is only a factor of 10^4; indeed, one critique of the colloidal glass transition as a model for molecular glass transitions is that the viscosity increase is not nearly as great. This discrepancy likely arises for several reasons. First, it is experimentally difficult to load high-volume fraction samples into a rheometer [66, 221]. Such a limitation can potentially be overcome using thermosensitive particles, which could be loaded into the rheometer at a temperature where the sample is liquid-like and then thermally changed to a higher volume fraction *in situ* [222, 223]. Second, ensuring that the sample has a well-known and controllable volume fraction can be extremely challenging [66]. Finally, colloidal samples that are sheared too rapidly can shear thin (the apparent viscosity decreases with increasing shear rate) or, at still higher shear rates, shear thicken (an increasing apparent viscosity with increasing shear rate). These trends are indicated qualitatively in figure 9. Shear thinning is more severe for $\phi > 0.5$ [28, 224], meaning that experiments at high ϕ must be done at extremely low shear rates ($\omega \to 0$ as described in section 2.5) and low applied stresses to see the correct linear response [178]. Measurements for $\phi \approx 0.6$ would take weeks or years to be done properly [221].

Important early work on the viscosity of colloidal suspensions was performed by Marshall and Zukoski using rheometry [28]. Their system consisted of small silica hard spheres (radius <300 nm) in a solvent of decahydronapthalene. A constant stress rheometer was used to measure viscosity at various applied stresses, enabling an extrapolation of the viscosity to a state of zero stress. For all particle sizes used, they observed an increase in viscosity with ϕ, with a sudden, apparently divergent increase at volume fractions associated with the glassy phase of hard spheres. They also found that the form of the increase was well described by the Doolittle equation,

$$\frac{\eta}{\eta_0} = C \exp\left[\frac{D\phi}{\phi_m - \phi}\right], \tag{15}$$

with $C = 1.20$, $D = 1.65$ and $\phi_m = 0.638$. This equation was first used to describe the temperature dependence of viscosity in molecular liquids approaching the glass transition [228]. The original Doolittle equation was expressed as a function of free volume (which was implicitly a function of temperature). We note that (15) has been modified in a reasonable fashion (see [28] for details) to depend on ϕ as shown above, with ϕ_m being the maximum packing. At $\phi = \phi_m$ in the above equation, the viscosity diverges. It is intriguing that their observed $\phi_m = 0.638$ is close to ϕ_{rcp}, where all motion is suppressed. Indeed, the data in figure 8 are also well fit by (15) with a similar ϕ_m [221]. This raises questions about whether the glass transition occurs at $\phi_g \approx 0.58$ or possibly at $\phi_{rcp} \approx 0.64$. We will discuss these questions more comprehensively in section 6, but for now, we note that the viscosity is large at ϕ_g and that other quantities, to be discussed next, diverge at ϕ_g.

The Doolittle model has been critiqued in the past as being oversimplified or perhaps founded on shaky physical arguments [229, 230], and it is possible that other functional forms would fit the data just as well [165, 221]. The question of which functional form is most appropriate is generic to studying the glass transition. It was noted by Hecksher *et al* in 2008 that multiple functional forms fit glass transition data (relaxation times as a function of T) [231, 232]. Of these expressions, some have a divergence at finite T while others have no divergence at all. In all cases, the experimental data range over many decades in η, but are clearly many more decades away from $\eta = \infty$, and so extrapolation is always tricky [233–235].

While the glass transition is associated with a dramatically increased viscosity, it is equally associated with a dramatically increased microscopic relaxation time and decreased diffusivity. For colloids, the long-time self-diffusion coefficient $D_L(\phi)$ approaches zero as $\phi \to \phi_g$ (see section 1.5 for a discussion of D_L). A related quantity is the intermediate scattering function $F(k_m, \tau)$, where the wave vector k_m is often chosen to correspond to the peak of the static structure factor. The decay time for $F(k_m, \tau)$ becomes large as the glass transition is approached, as shown in figure 5; this is the microscopic relaxation time scale, often termed τ_α when referring to the final decay of $F(k, \tau)$ [236]. (See section 2.4 for a discussion of DLS and scattering functions.) Roughly, $\tau_\alpha \propto a^2/D_L$, where a is the particle radius, and so both τ_α and D_L are considered measures of how microscopic dynamics slow near the glass transition.

The question then is how D_L and τ_α depend on ϕ [237, 238]. Results from viscometry and DLS studies were reported

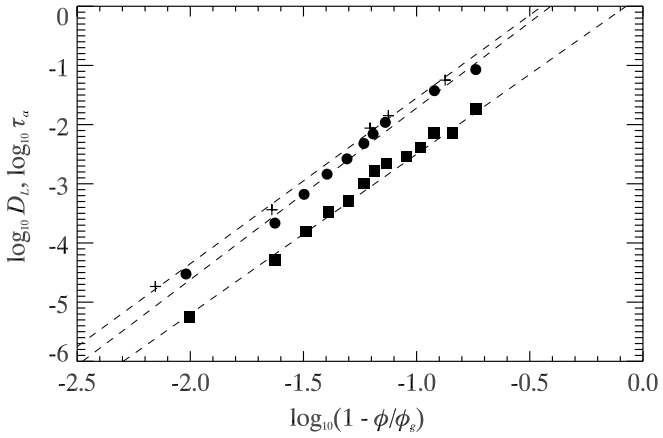

Figure 10. Growing relaxation time scale τ_α (plotted as $-\log(\tau_\alpha)$, circles) and decreasing diffusivity D_L (squares) plotted against the distance to the colloidal glass transition, using $\phi_g = 0.571$ for the D_L data and $\phi_g = 0.572$ for the τ_α data. Data taken from [100]. Diffusion constants are measured from figure 2(*b*) and τ_α from figure 5. Plus symbols are τ_α data from [247], a prior experiment by the same group.

by Segrè *et al* for a suspension of PMMA hard spheres over the range of volume fractions $0 \leqslant \phi \leqslant \phi_{\text{freeze}} = 0.494$ [239]. Intriguingly, they found that the growth of $\eta(\phi)$ (measured with a rheometer) was well matched by the growth of the inverse diffusion constant, $(D_L(k_m))^{-1}$. This suggests that at least to $\phi \approx 0.494$, viscosity and diffusion are well coupled. It is known that in molecular glasses, these two quantities can decouple: diffusion is quite slow, but not as slow as would be expected from measurements of η [236, 240–242]. van Megen *et al* acquired data up to $\phi_g - 0.01$ and found that D_L and τ_α remain well coupled; their data are shown in figure 10. Results for both η and τ_α from the same sample with $\phi > 0.494$ have not yet been obtained, partly because of the experimental difficulty of making the different measurements at exactly the same volume fraction [66, 243, 244]. Comparing data sets from different groups suggests that perhaps η and τ_α remain coupled [245], although such comparisons are non-trivial and the results should be treated cautiously [66]. In general, it is hard to accurately determine how $\eta(\phi)$ grows near ϕ_g or ϕ_{rcp}, partly because of the difficulty in measuring ϕ accurately, and partly because small changes in ϕ make a large difference, precisely as shown in figures 8 and 10. It is worth noting that some experimental differences between $\eta(\phi)$ and $D_L(\phi)$ may be due to slip at the particle surface [239, 246]. As already noted, another difficulty in measuring $\eta(\phi)$ for $\phi > 0.5$ arises due to the very slow shear rates required to do so—the need to shear at such low rates is itself evidence for a dramatically growing microscopic relaxation time scale [28].

Given the difficulties of doing both viscometry and DLS on the same samples, and given the power of DLS compared with viscometry, it is natural that many people have used DLS to examine how τ_α grows as $\phi \to \phi_g$. van Megen's group has performed well-known DLS experiments over three decades starting in the 1980s [32, 100, 142, 247–251]. One of their notable findings is that the increase in $\tau_\alpha(\phi)$ is well described by MCT; see, for example, [1, 247, 252, 253]. Significantly, not only is τ_α fit by MCT, but several other features of $F(k, \tau)$ are as well, with the only adjustable parameter being the scaling of the volume fraction ϕ.

The experiments by van Megen *et al* were performed with hard-sphere-like colloidal particles; parallel experiments were performed by Bartsch, Sillescu and co-workers starting in the 1990s, using softer colloidal particles [104, 105, 254–260]. Some intriguing differences were seen; for example, some relaxation processes still appeared to persist in the glass phase [105, 254]. Their early observations suggested a glass transition at $\phi \approx 0.64$ [104], but this was later attributed to depletion effects due to the likely presence of free polymers [256, 258]; see also the discussion in section 5.1. Later experiments by the same group found a glass transition at $\phi_g = 0.595$, which was higher than 0.58 likely due to the moderately high polydispersity of these samples (∼16%) [256]. Many of the predictions of MCT were confirmed in these soft particle experiments [105, 255], suggesting that the particle properties are not crucial.

The hard-sphere results have been recently updated by Brambilla *et al* who studied samples with $\phi > 0.58$ using DLS [261, 262]. Amazingly, they found that these slow and dense samples eventually equilibrated. Some of their results agreed quite well with the earlier work of van Megen *et al*. However, above ϕ_c, the volume fraction where MCT predicts a divergence of τ_α, they instead found finite values of τ_α—suggesting that these samples were not yet glasses and that ϕ_c of MCT is not equivalent to ϕ_g for their samples. These results are controversial [263–266]; key issues raised are difficulties determining volume fractions and difficulties comparing results with differing polydispersity [66].

It should be noted that there are other predictions of how $D_L(\phi)$ should behave near the colloidal glass transition. A notable theory taking into account hydrodynamic interactions is due to Tokuyama and Oppenheim [267, 268], which predicts a glass transition at a specific volume fraction $\phi_0 \approx 0.5718$ (with an exact expression given for this value).

Some understanding of how structure and dynamics relate to each other has been recently presented by van Megen *et al* [251, 269]. They studied sterically stabilized PMMA particles in decalin, which were well characterized to behave as hard spheres. In [251], they studied the MSD and identified the time scale $\tau_m^{(s)}$ at which the MSD had the smallest logarithmic slope, that is, the time scale at which the MSD was the most subdiffusive. Here the (s) superscript indicates self-motion. They also identified an analogous time scale for collective motion, $\tau_m^{(c)}(k)$, directly from DLS data, which was approximately the same as τ_m. These time scales both grow as the glass transition is approached, which makes sense. By examining the k dependence of $\tau_m^{(c)}(k)$, they showed that structural arrest—the slowing of the motion—starts at length scales corresponding to $1/k_m$, where k_m is the peak of the static structure factor, and then spreads to other length scales [251]. This suggests that as the glass transition is approached, the spatial modes of motion do not slow uniformly; that some are frozen out sooner. A related study by the same authors found that the dynamics exhibit qualitative changes for the metastable states, that is, $\phi > \phi_{\text{freeze}} = 0.494$ [269].

We refer the reader to [1, 72] for good reviews of experiments studying diffusion and relaxation times for the

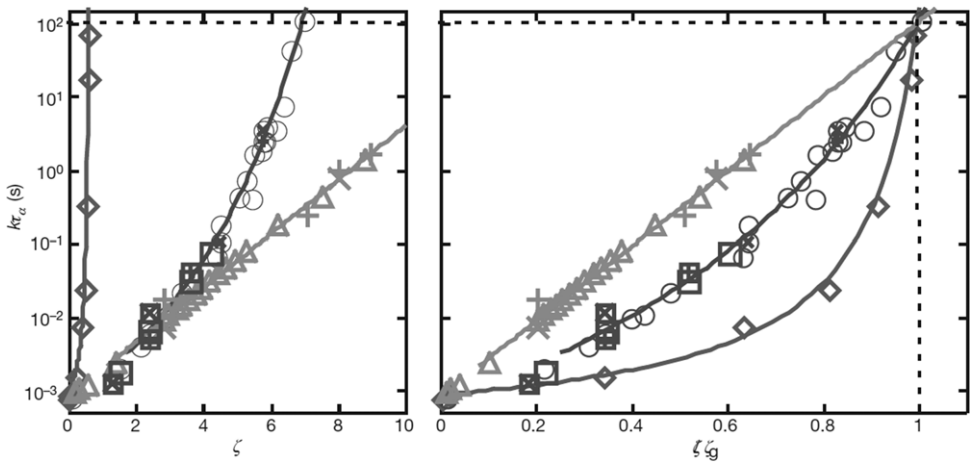

Figure 11. (*a*) Plot of scaled relaxation time $k\tau_\alpha$, where τ_α is measured from light scattering and k is chosen to collapse the data at low ζ values. Symbols are diamonds (stiff particles), circles and squares (intermediate stiffness), triangles (soft particles), crosses and pluses (rescaled shear viscosities from rheology measurements, corresponding to intermediate and soft particles, respectively). (*b*) Same data as (*a*), with the effective volume fraction ζ normalized by $\zeta_g \equiv \zeta(k\tau_\alpha = 100\,\mathrm{s})$. Reprinted by permission from Macmillan Publishers Ltd: *Nature* [276], copyright 2009.

colloidal glass transition, and how the experiments relate to MCT predictions. Earlier reviews summarize the state of these questions in 1998 [71] and 2001 [49]. MCT is specifically reviewed in [2, 270, 271].

3.2. Fragility

An important feature of molecular and polymer glasses is that, while the relaxation time scale grows dramatically in all cases, the *rate* of this growth varies between different samples. This difference is termed the *fragility* [3]. Fragile glass-formers are ones in which the relaxation time scale grows slowly over some range of the control parameter, and as the glass transition is approached, increases quite suddenly. Such glasses are 'fragile' in the sense that when their viscosity is high, a slight change in the control parameters (increasing T or decreasing P) results in a sharp decrease in the viscosity, easily 'breaking' the glassy behaviour. In contrast, 'strong' glasses exhibit Arrhenius behaviour, where time scales and viscosity grow smoothly and steadily as the glass transition is approached [6]. Results shown in figure 11(*b*) are from colloidal glasses and illustrate the types of behaviours one might see: here the straight-line data are from a strong glass, and the curved data correspond to fragile glasses.

The fragility can be defined in several ways. One common way is to fit the viscosity as a function of T to the Vogel–Tammann–Fulcher equation:

$$\eta/\eta_0 = \exp[DT_0/(T - T_0)]. \tag{16}$$

Here η_0 is the viscosity at large T, and T_0 results from a fit to where the viscosity would become infinite. The parameter D is called the 'fragility index', and is larger for stronger glasses; $D \to \infty$ corresponds to Arrhenius behaviour. For fragile polymer glasses, D can be as low as $\sim$2 [3]. This non-Arrhenius behaviour is taken as a sign that molecules cooperate in their motion; diffusion and structural relaxation are no longer local processes [272]. For colloids, one might exchange T_0/T with ϕ/ϕ_0, given that for regular glasses one decreases T to T_g and for colloids one increases ϕ to ϕ_g. Thus colloids would be fit with the Doolittle equation (15) with $C = 1$:

$$\eta/\eta_0 = \exp[D\phi/(\phi_0 - \phi)]. \tag{17}$$

Using this definition, hard-sphere colloids appear to be fragile glass-formers with $D \approx 1.15$ (from figure 8 [221]) or $D \approx 1.65$ (from rheology [28]). Equivalent formulas can be written using τ_α/τ_0; light scattering data on hard-sphere-like colloids suggest $D \approx 0.50$ [202, 261, 262]. However, the exchange of T_0/T with ϕ/ϕ_0 is perhaps misleading [272]. In [272], Berthier and Witten argue that ϕ is more analogous to energy density, and that the non-dimensional pressure $1/Z = PV_p/\phi k_B T$ is more analogous to $1/T$, using pressure P and particle volume V_p. As P has a non-trivial ϕ dependence, they point out that the relationship between η and ϕ can be confusing when comparing different types of colloidal particles, especially as Z is generally not easily measurable in an experiment. Overall, however fragility might be defined, an important question is 'what features of a glass-forming material relate to the fragility?' [202, 273–275].

This question has recently been explored by Mattsson *et al* [276] with colloidal suspensions of soft hydrogel particles. These particles easily deform and so can be compressed as their concentration is increased; for this reason, their glass transition does not occur at the same volume fraction of $\phi_g \approx 0.58$ as for hard particles. The authors considered a generalized volume fraction $\zeta = nV_0$, where n is the particle concentration and V_0 is the volume of an undeformed particle. Given that particles can be compressed to much less than V_0, the generalized volume fraction ζ can greatly exceed 1. Shown in figure 11, Mattsson *et al* found that softer particles (triangles) behaved as strong glasses, while harder particles (circles, diamonds) behaved as more fragile glasses, using the equivalence between $1/T$ and ζ. This is an exciting demonstration of a model colloidal system which

can be used to explore fragility. However, an open question is whether using the non-dimensional pressure Z would perhaps collapse the data between the differing particle types [272]. The simulations of [272] show that hard spheres are 'fragile' when plotted against Z.

The results of Mattsson *et al* are interesting, but it is not completely clear how particle softness relates to fragility. A simulation of different particle potentials did not find any fragility changes [277], although this study only considered varying T rather than density. Certainly for polymer glasses, fragility can be quite different depending on if T or density is varied [275]. Furthermore, 'softness' has two distinct meanings. In simulations such as [277], softness refers to the shape of the interparticle potential. Often the repulsive part of the potential decays as $1/r^n$, and smaller values of n are considered softer particles. In contrast, Mattsson *et al* used softness to refer to the particle modulus [276], which probably is a prefactor to an interparticle potential with fixed shape.

A recent mode-coupling study suggests that both the shape of the potentials and their prefactors may be needed to understand Mattsson *et al*'s results [278]. For example, if the interparticle potential is $\sim 1/r^2$ at large separations r, and $\sim 1/r^6$ at smaller separations, then increasing particle concentration can shift the scale of the interaction energy to a different regime of the potential. If such an effect was properly accounted for, all of the data might collapse for different softnesses [59]. In a sense, this suggests that the results for the soft spheres can be considered in terms of their effective hard-sphere size [279, 280], thus explaining the results in terms of a mapping from ζ to $\phi_{\text{effective}}$ [59, 281, 282]. However, the functional form of the interparticle potential is unknown for hydrogel particles. Furthermore, it is not known if or how the interparticle interactions vary between different batches of Mattsson *et al*'s particles. (Other groups have noted that their particles vary from batch to batch: see the discussion in [282] comparing their results with their prior work in [283].) While the results of Mattsson *et al* are exciting, they raise many questions. A full understanding requires either precise knowledge of how hydrogel particles interact or insights from simulations on how to replicate the experimental data.

One can also consider the results of Mattsson *et al* in another way. The Arrhenius ζ-dependence for the softer particles suggests that the energy barrier for rearrangements is independent of ζ. Perhaps soft particles can rearrange without significantly affecting others, and so rearrangements involve only a few particles. In contrast the harder particles might exhibit growing dynamical heterogeneity (see section 3.3), requiring more and more particles to rearrange, and thus leading to a growing energy barrier with ζ. If these conjectures are true, this would suggest that soft particles are not effectively hard particles with a different radius. Microscopy experiments may be able to shed light on the question of particle rearrangements.

Recent simulations suggest different ways to tune the fragility of colloidal systems. One simulation showed that fragility was tunable using a binary system and controlling the size ratio and number ratio of the two species [202]. While intriguing and potentially useful for tuning the properties of colloidal suspensions, a binary system would be of limited use for understanding the fragility of single-component molecular glasses. Another simulation studied soft particles with finite-range potentials, quite analogous to soft colloidal particles, and found that the temperature-dependent fragility increased dramatically when the particles were over-compressed (density increased above the point where the particles had to interact) [272, 280].

3.3. Dynamical heterogeneity

In a liquid below its melting point, some regions may exhibit faster dynamics than others even though, spatially, these regions may be very close [236, 284, 285]. This behaviour is called *dynamical heterogeneity*, and illustrates that different regions of a system relax at different rates. In such a system, relaxation time scales and length scales are coupled, that is, longer relaxation times are typically associated with larger collections of particles. One key idea here is that of cooperative motions [286]: near the glass transition, perhaps molecules need to 'cooperate' in order to rearrange.

Cooperative motion has been seen in colloidal samples, such as the one shown in figure 12. The left image shows a raw confocal microscope image, a 2D slice through a 3D sample at $\phi = 0.46$. The right image shows the difference between particle positions in the left image and an image taken 60 s later. Some regions of this image are grey, indicating places where particles move relatively little during this period of time. Other regions are black and white, indicating groups of particles all moving together. For these groups, motion is from black to white; for example, the anomalously large particle moves slightly to the left. It can be seen that in general, neighbouring particles that are rearranging tend to move in similar directions. This sample is relatively far from the glass transition (the images come from a sample with $\phi = 0.46$ as compared with $\phi_g = 0.58$ for these experiments). As the glass transition is approached, the regions of rearranging particles grow larger, but the displacements during a given rearrangement are smaller [137], so similar images at larger ϕ are less revealing. Overall, observations of spatially heterogeneous motion have been seen with microscopy in several colloidal experiments [110, 112, 128, 129, 287–289].

The interpretation of these results relate to cage trapping and cage rearrangements. As described in section 1.5, at short times, particles move due to Brownian motion, but this motion is constrained because particles collide with their neighbours. The neighbours thus 'cage' the particle—of course, the particle is also part of the cage around its neighbours [2, 93–98]. On longer time scales, the cages relax and the system rearranges. As figure 12 shows, rearrangements often occur when one particle moves, another particle follows, and so on.

As the glass transition is approached, the size of the cooperative groups of particles increases, as well as the time scale for these motions [99, 128, 129, 137, 290]. The growing length scales (quantified from spatial correlation functions) extend up to ~4–5 particle diameters [198, 290], shown by circles in figure 13. Rearrangements can involve up to ~ 200 particles [129], and the average size of a rearranging region

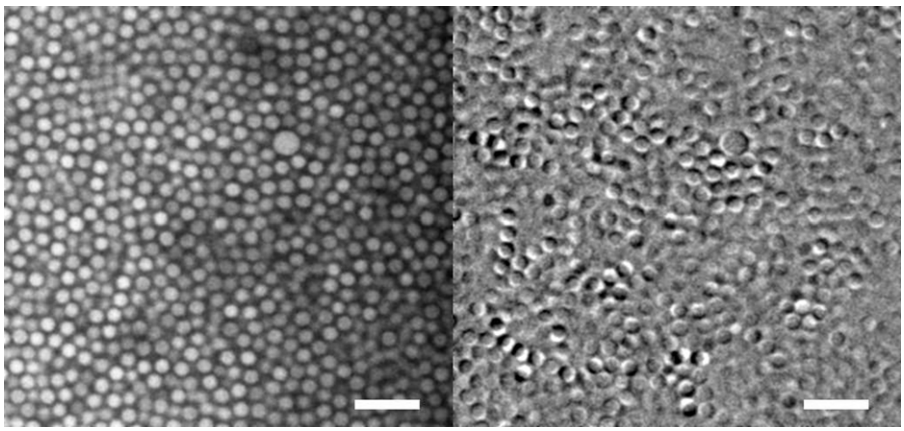

Figure 12. Left: confocal microscope image of a sample with $\phi = 0.46$. Right: difference between the left image and one taken 60 s later. Where this image is grey, nothing has moved; where it is black, a particle existed at the earlier time, and where it is white, a particle existed at the later time. Of course, particle motion also occurs perpendicular to the plane of the image. In both images, the scale bar indicates 10 μm. For this sample, the particles are slightly charged, shifting the onset of freezing from $\phi_{\text{freeze}} = 0.494$ to $\approx$0.42 [48].

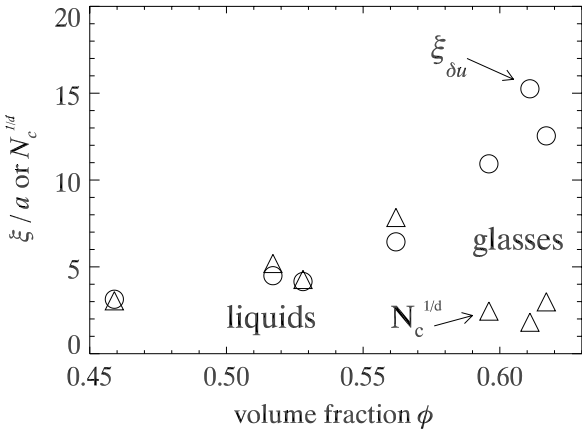

Figure 13. Data on growing length scales for dynamical heterogeneity in colloidal samples. Circles: length scales $\xi_{\delta u}$ found from spatial correlations of mobility, normalized by particle radius $a = 1.18\,\mu$m [290]. Triangles: mean cluster size in terms of number of particles N_c, converted to a length scale using the fractal dimension $d = 1.9$ [129]. These are clusters of mobile particles as defined in [129], and by computing $N_c^{1/d}$ we find the typical length scale of such clusters. The same data were analysed in [129, 290]. For these experiments, the glass transition was identified as $\phi = 0.58$.

is indicated by triangles in figure 13. Intriguingly, for liquid samples ($\phi < 0.58$), these two length scales are essentially identical. For glassy samples, the correlation length scale is large, but cluster sizes are small. This is probably due to difficulty defining cluster sizes in glassy samples as discussed in [291]. Rearranging particle displacements are small and can be lost in the 'noise' of particles diffusing within their cages in a glassy sample. More careful analysis reveals larger clusters in glassy samples, although the details of defining such clusters are ambiguous in glasses due to ageing [291]—see the discussion in section 4.2.

These experimental observations of spatial dynamical heterogeneity are in good agreement with prior observations in computer simulations [56, 194–196, 198–200, 204, 292]. While the increasing size of these cooperative regions is a striking observation, it is a bit unclear exactly how this relates to the growing relaxation time [197, 293]—is it a cause, effect, or side-effect? Intuitively, it makes sense that if more and more particles need to move simultaneously in some coordinated fashion, that this is hard to do and will occur less often, thus connecting directly to slowing time scales for diffusion. In this sense, dynamical heterogeneity and the glass transition are strongly connected, and the former could be said to 'cause' the latter. Some evidence for this comes from simulations which see diverging measures of dynamical heterogeneity [196, 292, 294, 295]. One intriguing recent result comes from simulations of a 4D hard-sphere system: there a glass transition was seen, but dynamical heterogeneity was much less significant [208]. This suggests that perhaps glassy behaviour can occur for other reasons. (As noted in section 2.6, in general similar phenomena are seen in two dimensions and three dimensions, and one would assume that a 4D simulation can still provide useful insight into the 3D problem.)

It would be useful to understand the factors that allow some particles to rearrange, or conversely the factors that prevent the other particles from doing so. It has been noted that higher local volume fractions are weakly correlated with reduced mobility [137, 296, 297]. The correlation is sufficiently weak that it has essentially no predictive ability. Simulations, though, have shed some light on this. Widmer-Cooper *et al* conducted simulations that showed some regions within a sample have a higher 'propensity' to rearrange [203, 216]. To come to this conclusion, they ran repeated simulations beginning with the same initial particle configurations. From the initial configuration, the system was evolved using molecular dynamics and randomizing the velocities of the particles. Although again, these sites were only weakly correlated with structural properties [203, 216, 298, 299]. Such a procedure has not yet been tested in a colloidal experiment. Investigating dynamical heterogeneity is a good example where simulations are quite powerful; simulations preceded and guided the experimental data analysis [204], and allow for studies that are experimentally difficult or even impossible [203, 208].

Figure 12 shows clear spatial variations in mobility. However, another mode of studying dynamical heterogeneity

is to consider the temporal fluctuations of mobility: in any given region, the amount of motion will fluctuate in time [67, 291, 300]. These fluctuations can be quantified with a four-point susceptibility function called χ_4 [294, 295, 301–303]. This function has been shown to be closely related to the cooperative motion discussed above, and can be used to pick out a time scale corresponding to the dynamical heterogeneity. The analysis has been successfully applied to colloidal experiments several times [301, 304–306], with the results essentially in agreement with what has been seen in simulations.

One could argue that studies of glassy systems should focus on understanding the behaviour of slow particles, rather than fast ones. After all, over a given period of time the overwhelming majority of particles in a glassy system are fairly immobile. By studying mobile particles, one learns how mobility decreases as the glass transition is approached—for example, particle motions are not only rarer, but also smaller [137]. Also, it is usually the case in experiments that faster moving particles are easier to distinguish. However, one confocal microscopy study focused its analysis on less mobile particles [167], finding that clusters of slow particles percolate through a colloidal glass.

Dynamical heterogeneity in molecular glass experiments is reviewed in [236, 284, 285]. Additionally, a chapter in [162] gives a lengthy review of dynamical heterogeneity in colloidal glasses. An earlier review of dynamical heterogeneity in soft glassy materials is [151].

3.4. Confinement effects

Phase transitions are usually investigated in the context of macroscopically large systems. However, confining samples so that one or more dimensions are microscopic leads to new physics, including confinement-driven phases [307]. For amorphous phases, the glass transition temperature T_g is often changed by confinement [308–318]. In some experiments, the glass transition temperature is decreased upon confinement (as compared with the transition temperature in bulk) [57, 209, 312, 313], whereas in others, the glass transition temperature increases [209, 308, 310, 319]. In some cases, T_g can increase or decrease for the same material, depending on the experiment [209, 308, 313, 317]; this is likely due to differing boundary conditions [308]. In molecular glass experiments, important differences are found when studying confined samples supported by substrates, as compared with free-standing films [308, 315–317]. In other experiments, results depend on whether the confining surface is hydrophobic or hydrophilic. Computer simulations indicate that confinement influences the arrangement of atoms [57, 209, 210, 320], which might in turn relate to the change in the glass transition temperature. However, it is difficult to probe the structure and dynamics of nano-confined materials.

Colloids thus can serve as an excellent model system for studying confinement effects. Such experiments have been performed by two groups who confined samples between parallel glass plates [213, 321]. Nugent *et al* used a binary sample to prevent crystallization [213], while Sarangapani and Zhu studied a monodisperse sample [321]. Both experiments used confocal microscopy to observe a dramatic slowing down of particle motion in samples that were very confined. This suggests that the glass plates act analogously to 'sticky' boundaries in the molecular glass experiments conducted on substrates, which also find a slowing down of particle motion [308]. Follow-up work showed that rough confining surfaces slowed motions even further [215]. The experiments show a clear connection between layering of particles against the walls and their mobility [213], which has also been studied by simulation [57, 322, 323].

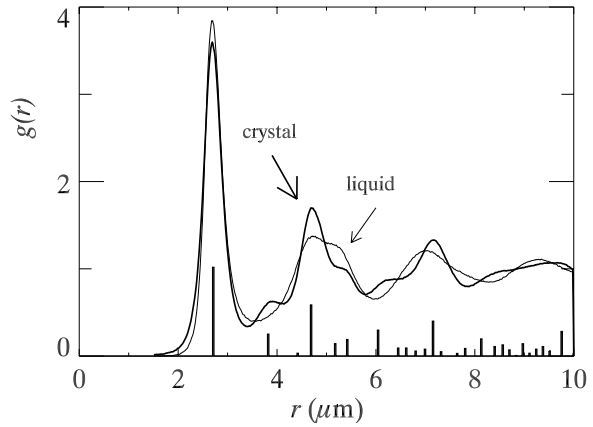

Figure 14. Pair correlation function $g(r)$ for a liquid sample ($\phi = 0.48$) and a crystalline sample ($\phi = 0.57$), with particle radius $a = 1.18\,\mu$m. The particles are the same colloidal PMMA spheres used in [129], and were observed using confocal microscopy. For perfectly hard particles, the position of the first peak in $g(r)$ would be at $2a$. Here, however, the position of the first peak is at $\sim 2.7\,\mu$m, larger than $2a = 2.36\,\mu$m, because the particles are slightly charged. The vertical bars at the bottom edge of the graph are the positions of the peaks of $g(r)$ for an ideal random hexagonal close-packed crystal. Properly speaking, these should all be Dirac delta functions (infinitely high); here they are truncated by finite resolution, and rescaled but still proportional to their magnitude in the ideal case. The peaks of the experimental crystal are broadened due to Brownian motion around the particles' lattice sites, a slight polydispersity and also particle-tracking uncertainty.

4. Features of glassy systems

4.1. Amorphous solids

It is visually apparent from the bottom of figure 1 that colloidal glasses and crystals have different structures. Repeating patterns, like those in a crystal, are completely absent in the glassy state and instead the glass more closely resembles a very dense liquid. Although liquid-like, the system is dense enough that it can bear some degree of stress over short time periods and respond elastically (see G' in figure 7(a)). Thus, glassy systems are commonly described as *amorphous solids*.

A simple measure of structure is the pair correlation function (or radial distribution function), $g(r)$, which describes fluctuations in particle number density at a distance r away from a given particle. The pair correlation functions for a colloidal crystal and a colloidal liquid are shown in figure 14. The curve for the crystal (bold line) has fluctuations at definite positions, corresponding to spacings between particles in

the random hexagonal close-packed lattice. If this were an ideal crystal, these fluctuations would be narrow spikes, but in figure 14 they are broader due to Brownian motion, polydispersity, and particle-tracking uncertainties, all of which ensure that particle positions are not on exact lattice sites. The liquid curve (thin line in figure 14) differs significantly from the crystal, reflecting that the sample itself has much less structure. The second peak for the liquid, around $4 < r < 6\,\mu$m, is slightly split into two sub-peaks. As can be seen, these correspond to two features of the crystal curve. The origin of the sub-peaks is local packings of three or four particles that appear crystalline and result in spacings of second-nearest-neighbour particles that correspond to the crystalline spacings. In some experiments, this split second peak of $g(r)$ is more obvious, and sometimes taken as a signature of the glassy state; however, this is not a defining feature but merely a common observation.

In 1991, Snook *et al* used SLS to study the structure of colloidal glass samples [54]. Comparison with simulations of random close-packed spheres confirmed that the experimentally obtained colloidal glass was indeed amorphous. Later in 1995, van Blaaderen and Wiltzius used confocal microscopy to examine the amorphous structure of a colloidal glass [127]. They studied quantities such as the number of nearest neighbours, bond-order parameters, and $g(r)$, and found that all were in good agreement with simulations of random close packing [127]. More recently in 2010, Kurita and Weeks used sedimentation to obtain a random close-packed sample and imaged nearly half a million particles (using confocal microscopy), again finding that the experimental sample was quite similar in many respects to simulations of random close packing [324]. Their large sample size enabled a comparison with recent simulations which found 'hyperuniformity,' meaning that density fluctuations disappear linearly with wavelength in the long wavelength limit [325]. An implication of a sample being hyperuniform is that it is incompressible, which has been conjectured to be a requirement for random close-packed systems [326]. The only disagreement with simulations was that the experimental density fluctuations did not go to zero at long wavelengths, implying that the sample was compressible. However, recent simulation results suggest that the disagreement is due to polydispersity in the experimental sample [327–329]. Re-analysis of the Kurita and Weeks data found that accounting for polydispersity does indeed demonstrate that the experimental samples are hyperuniform, and thus incompressible [330]. However, liquids and glasses have a finite compressibility: these observations of incompressibility in random close-packed samples, then, demonstrate a structural difference between such samples and liquids and glasses. This shows the limits of such samples as models for liquids, which is intriguing given that random close-packed hard spheres are one of the original models for liquids [34].

4.2. Ageing

As with their molecular and polymer counterparts, colloidal glasses exhibit *ageing*—as the system evolves towards equilibrium, measured properties may change with time [80, 164, 331–335]. In a sense, ageing can be thought of as a transient effect: consider a supercooled fluid whose temperature is decreased slightly from T_1 to T_2. If the relaxation time scale at T_2 is τ_2, then equilibration to the new temperature occurs over a period $\sim\tau_2$ [336]. During the equilibration process, the dynamics depend on the waiting time t_w since the temperature was changed to T_2. These t_w dependent dynamics are ageing, and if τ_2 is sufficiently large, then the sample can be considered a glass which will age for as long as an experiment is performed [337]. In contrast, for supercooled liquids the same ageing phenomena are seen, but only for $t_w \lesssim \tau_2$; here, the phenomena might equally well be described with the word 'equilibrating' [80].

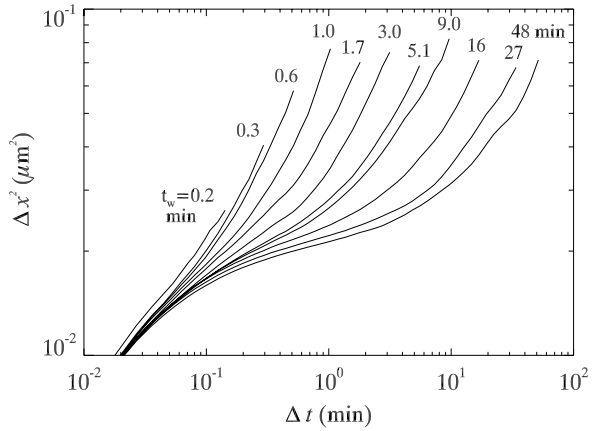

Figure 15. The MSD for an ageing colloidal sample. The waiting time is labelled for each curve. Data from [291], corresponding to a sample with $\phi \approx 0.62$ observed with confocal microscopy. Note that each curve is averaged over a window of time centred on the t_w indicated; see [291] for details of this window averaging. The curves are evenly spaced in $\log(t_w)$, but not evenly spaced on the graph, reflecting the fact that within the imaged region ($\sim$1000 particles), ageing takes place intermittently [300, 340].

Ageing is readily observed in colloids by examining the MSD at different waiting times, t_w, where the waiting time is defined as the time since the last perturbation. The system in figure 15 displays a slowing of dynamics as t_w is increased (with $t_w = 0$ defined as the end of an initial stirring, see below) [291]. The short time dynamics are unchanged and reflect particles diffusing within their cages. But with increasing t_w, the plateau broadens and the upturn occurs at longer Δt, indicating that relaxation occurs over increasingly larger time scales. Analysis of these data found that particle mobility was related to $\log(t_w)$ [338]. Analysis of light scattering data, in contrast, found time scales for motion which depended algebraically on t_w [335]. For all of these experiments, ageing occurs over the entire duration of the experiment, and so these samples are easily classified as a glass. There is recent evidence, though, that even fairly dense colloidal samples can eventually equilibrate given enough time, raising questions about how to best define ϕ_g [261, 339].

In molecular or polymer glasses, vitrification occurs when the temperature is quickly lowered, namely the system is thermally quenched. In colloids, the creation of glassy systems typically involves slow centrifugation of a sample. Hence, the

time at which the system becomes glassy is poorly defined. To this end, the study of colloidal glasses often begins with a process known as *shear rejuvenation* in which the system is stirred or sheared in order to remove any history dependence [341–345]. The hope is that vigorous stirring breaks up any subtle structure in the sample so that experiments begin with a randomized initial structure. The time that the stirring stops defines $t_w = 0$ [146]. Subsequent ageing, then, is presumably a slow evolution of the structure to some 'older' state [346]. There is evidence that in some cases the shear rejuvenation process produces different types of behaviour than those observed in polymer glasses that are thermally quenched [345, 347, 348].

A process more analogous to a thermal quench would be to increase the volume fraction from ϕ_1 to $\phi_2 > \phi_1$. This is possible with hydrogel particles, whose size is controllable by temperature (see section 5.1). To date, there have been several important ageing experiments using these particles. Purmono *et al* studied the rheological behaviour of ageing hydrogel samples [345, 349]. They found that both shear rejuvenation and changing the volume fraction resulted in reproducible initial states, although they were slightly different. Subsequent microscopy experiments by the same group used tracer particles to confirm and extend these results [350]; in particular, the sample was revealed to be spatially dynamically heterogeneous, with mobile and immobile particles coexisting. Other experiments by this group demonstrated that ageing behaviour was independent of particle softness, despite the glass transition depending on both volume fraction and particle softness [351]. In another experiment, Yunker *et al* studied dynamical heterogeneity during the ageing of a quasi-2D sample and found that the size of rearranging regions increased as the sample grew older [111]. These results contrast with earlier work done in three dimensions with a shear rejuvenated sample [291]; differences in dimensionality and quench method are both plausible explanations for the different observations. In another hydrogel experiment, Di *et al* [352] replicated certain classic ageing experiments [353, 354]. For example, in 1964 Kovacs found that molecular glasses quenched to T_2 from $T_1 > T_2$ would approach equilibrium differently than if heated to T_2 from $T_3 < T_2$. Di *et al* observed the same 'asymmetric approach' using hydrogel particles observed with DWS (see section 2.4).

A natural question to ask is 'are there structural signatures of ageing?' That is, given information about the structure of two samples, is there some quantity that distinguishes an 'old' sample from a 'young' one? Indeed, it is somewhat intuitive to expect a correlation between ageing dynamics and structure. In polymer glasses, for example, systems become denser as they age [355]. For a colloidal glass composed of hard-sphere-like particles, presumably the only 'clock' in the sample is the structure; the sample should have no other way of knowing t_w. The relevant quantity in colloidal glasses, however, has remained elusive. Cianci *et al* [346, 356] searched for correlations between the structure and dynamics of an ageing colloidal glass, specifically looking at four-particle tetrahedral configurations within the system. A wide range of structural parameters were examined but none changed with t_w. However, ageing did occur intermittently [300, 357] via spatially localized groups of particles [146, 291], similar to what has been seen in simulations [334, 358–360]. These slightly more mobile particles were associated with more disordered local environments [346]. Presumably the more mobile particles are the ones that change the structure and thus are responsible for the sample having a larger age, but the connection between structure, dynamics and age remains unclear [346]. A similar set of observations was found by the same group studying a binary sample: local composition, quantified by relative numbers of small and large particles, influenced dynamics but did not itself change as the sample aged [146]. These colloidal observations are in reasonable agreement with simulations, which found that structural changes during ageing are quite subtle [333, 361]; they also agree correlations between structure and mobility in other simulations and experiments [137, 362, 363].

Ageing has also been considered in regard to the fluctuation–dissipation theorem [364], which connects temperature, viscous friction and interparticle potential to diffusive motion. In the absence of interparticle potentials, as in the case of hard-sphere particles, fluctuation–dissipation can be written simply as

$$D = \frac{k_B T}{C}, \tag{18}$$

where C is a viscous drag coefficient. The drag force on a sphere moving at velocity v is $F_{drag} = Cv$ (see (8)). Therefore, by measuring the velocity v of a sphere feeling a known external force, and measuring D for the same sphere with no external force, one can calculate T. In the same way that MSD has a non-trivial dependence on lag time Δt and waiting time t_w (as shown in figure 15), so D can be considered to be a function of frequency ($\omega \approx 2\pi/\Delta t$) and t_w, and likewise the relationship between F_{drag} and v may have non-trivial frequency dependence [174]. The ratio of these quantities can be generalized to provide an effective temperature, T_{eff} [364]. This idea has been tested in a wide variety of non-equilibrium situations, including sedimentation experiments [365], simulations of a sheared foam [366], granular experiments [367, 368], simulations of glasses [334, 369], experiments with regular glasses [370, 371] and experiments with colloidal glasses [245, 357, 372–375]. For hard-sphere colloidal glasses, the calculated effective temperature is a few times greater than the actual temperature [245, 374]. Although this may seem counter-intuitive, the observation can be rationalized by arguments from statistical mechanics. Temperature is essentially a measurement of the width of the distribution of energy states. One can think of particle rearrangements as the exploration of various energetic configurations available to the system: for low to moderate ϕ, rearrangements are easy and the fluctuations in energy from one configuration to the next are small; for $\phi \approx \phi_g$, rearrangements require cooperative motion between many particles and therefore larger energy fluctuations. As the energy distribution is broader for $\phi \approx \phi_g$, this automatically implies a higher effective temperature. Thus, the measured

T_{eff} is related to cooperative motion and large scale structural rearrangements within the glass [374]. Although the effective temperature is larger than T, it was also found that T_{eff} does not seem to change with age [374].

Recent experiments with magnetic particles [376] allow the possibility of doing experiments with an ultrafast effective concentration quench. These particles have a repulsion that is controllable with an external magnetic field, and so their effective size can be rapidly varied. This enables experiments to study ageing at extremely short time scales after the quench.

4.3. Shear of colloidal glasses

So far, this review has discussed equilibrium properties of supercooled colloidal fluids and out-of-equilibrium ageing in colloidal glasses. Another way to push a sample out of equilibrium is to apply shear, for example using a rheometer (see section 2.5). The interplay of ageing and shear have been studied by several groups [377–379], and as discussed in section 4.2, shear is often used by colloidal scientists to 'rejuvenate' an ageing sample [291, 341–343]. In this section, we will briefly summarize some of the key results that have been found when shear is applied to colloidal liquids and glasses.

One question to be asked is 'how quickly is the sample sheared?' This is quantified by the non-dimensional Pèclet number [380]. This number can be thought of as the ratio of two time scales. The first is the time scale τ_{D} a particle takes to diffuse its own radius a, defined in (5). The second time scale is the inverse of the strain rate, $\tau_{\text{S}} = (\dot{\gamma})^{-1}$, which is the time it takes for a particle to be sheared a distance equal to its own radius, relative to another particle in an adjacent shear layer. Thus the Pèclet number is given by

$$Pe = \frac{\tau_{\text{D}}}{\tau_{\text{S}}} = \frac{\pi \dot{\gamma} \eta a^3}{k_{\text{B}} T}. \tag{19}$$

This assumes that diffusion is well described by the physics in section 1.5 (see (3)–(5)). More relevantly for colloidal glasses, the long-time diffusion sets the time scale [174, 380]: in other words, the time a particle takes to diffuse a distance a is much slower than in a dilute sample. In this case, the modified Pèclet number can be defined in terms of the long-time diffusion constant D_{L} as

$$Pe^* = \frac{\dot{\gamma} a^2}{6 D_{\text{L}}} \tag{20}$$

(compare with (5)). If $Pe^* < 1$, then diffusion is more important for rearranging particles, whereas if $Pe^* > 1$, then shear rearranges particles before they can diffuse an appreciable distance. Thus, if one intends to understand shear-induced behaviours, it is necessary to shear quickly (high Pe^*) so that diffusion has insufficient time to equilibrate the system. In contrast, the measurements of $\eta(\phi)$ in section 3.1 wish to avoid shear-induced effects altogether, and so samples are sheared extremely slowly (low Pe^*).

The other question is how large a strain should be studied. For small strains, the rheological behaviour is linear [163]; that is, the viscoelastic moduli do not depend on the strain amplitude (see section 2.5). Early measurements, such as those in figure 16, found that only above a critical strain $\gamma_{\text{c}} \approx 15\%$ does a colloidal glass sample show significant plastic rearrangements [381, 382] (a later experiment using confocal microscopy lowered this to $\gamma_{\text{c}} \approx 8\%$ [383]). This result supports the idea that a colloidal glass has a yield stress, that is, it is a solid. The elastic response of the sample strained less than γ_{c} has been attributed to a distortion of the nearest-neighbour cages surrounding particles (see section 3.3 for a discussion of cages). Equivalently, it can be thought of in terms of free energy; in an unstrained sample, particles are packed randomly in some structure that maximizes entropy and minimizes free energy. When strained, particles move away from that structure at a cost to free energy. So for small strains, the sample gives a linear, elastic response. Above γ_{c}, particles break free of their cages and can rearrange [166, 189, 380–382]. (Although, it is possible that a large region can shift without particles being uncaged in the interior [384].) To some extent, particle rearrangements occur for smaller strains, but may be thermally activated in those cases [385].

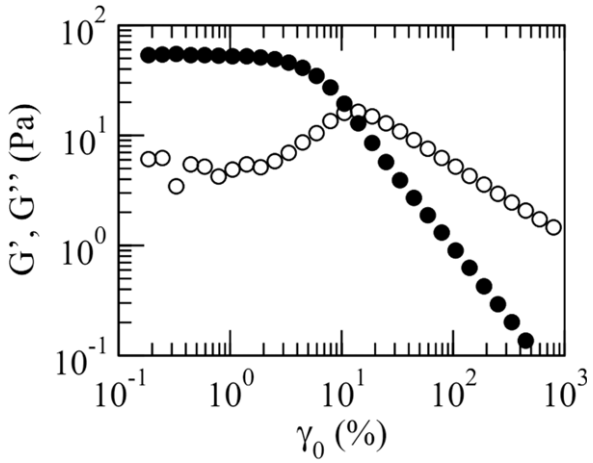

Figure 16. Elastic modulus (G'—filled symbols) and loss modulus (G''—open symbols) as a function of strain for a colloidal glass with $\phi = 0.645$. The sample here has a polydispersity of ≈12%, hence the large ϕ. Squares correspond to a slow strain rate ($f = 1\,\text{rad}\,\text{s}^{-1}$) and circles a high strain rate ($f = 100\,\text{rad}\,\text{s}^{-1}$). Reprinted with permission from [381].

Several works have noted that strained systems show dynamically heterogeneity, similar to the thermally activated rearrangements in supercooled colloidal liquids discussed in section 3.3. In other words, the particles that undergo plastic rearrangements in a sheared sample are distributed non-uniformly in space. This has been studied in experiments [380, 383, 385–389] and simulations [201, 388, 390, 391], and was originally predicted by theory [392]. One question that has been raised from studying the shapes of these regions of rearranging particles is 'are these rearranging regions oriented in any particular fashion relative to the shear?' A sheared sample has three unique directions: the velocity direction; velocity gradient direction; and vorticity direction (perpendicular to the first two). Particle motions differ trivially along the velocity gradient direction, and these overall affine motions can be subtracted from the observed particle motion in a confocal microscopy experiment [139, 387]. Some confocal

microscopy observations found that diffusion is isotropic [380, 387] and that the shapes of the rearranging regions are likewise isotropic [380]. However, simulations suggest that particle motions and rearrangements are not isotropic when sheared in the nonlinear regime [391]. Recent experiments confirm that with the right analysis techniques, anisotropic rearrangements are seen, with long-range correlations due to elastic effects [389]. In general, there are a variety of ways to define and identify plastic rearrangements in a sheared sample; these definitions are compared and contrasted in [380]. The sizes of the dynamically heterogeneous regions appear to be smaller in a sheared sample as compared with the unsheared sample [201, 388].

On a more macroscopic scale, a manifestation of spatially heterogeneous motion is *shear banding* [393–395]. Often when shearing complex fluids, the majority of the strain occurs within a narrow band of the sample, with the rest of the sample remaining relatively unstrained [393–398]. Hence, a measurement of viscosity which assumes uniform flow will lead to incorrect results. Shear banding has been observed and studied in dense colloidal suspensions in recent years [378–380, 389, 399–401] and presented problems for rheology for much longer [188]. The origins of shear banding in complex fluids continue to be an active research problem [402].

Given the industrial importance of shearing dense complex fluids, it is unsurprising that the shear behaviour of many different types of complex fluid glasses has been studied. Examples include emulsions [403], soft colloids [404], star polymers [405], colloidal gels [406] and attractive colloidal glasses [407] (see section 5 for the distinction between a colloidal gel and an attractive colloidal glass [408]).

There has also been a fair bit of theoretical work studying the flow of glasses and glassy complex fluids [222, 392, 409–412]. Some of these are MCT analyses, which do a good job describing shear of dense colloidal suspensions near the glass transition [410, 222]. Other theoretical work examines the flow of polydisperse glassy complex fluids [411, 412]. A key prediction of this theory is that a sample will initially build up stress elastically. After some time, a local plastic event occurs and the stress is redistributed in a non-local fashion around the location of the plastic rearrangement. Thus the ability of a local region of the sample to flow depends on what is happening in adjacent regions. This may potentially explain shear banding [412] and other observations of flow profiles in a variety of complex fluids [411, 413, 414].

5. Other soft glassy materials

So far, this review has focused on the colloidal glass transition and experimental work on hard-sphere-like colloidal particles, such as those used in the earliest experiments [30, 142, 248]. We briefly mention here other soft materials that are used for glass transition studies.

5.1. Soft colloids, sticky particles, emulsions and foams

Several groups study colloidal glasses composed of polymer hydrogel particles, which interact via a soft repulsion [104, 105, 111, 223, 254–256, 258, 276, 281, 282, 352, 415–417]. These particles can be packed to volume fractions above $\phi_{\rm rcp}$ of hard spheres, with potentially interesting consequences (see section 3.2). The stiffness of the particles can be controlled by the amount of cross-linking or using hard cores with hydrogel shells. The size of these particles can be varied by controlling the temperature or pH [418]. Compressed particles are harder, while swollen particles are softer: this allows for the same particles to be used to test how particle softness influences behaviour [276] and to look for general trends [223, 417]. The temperature dependence provides a simple way to tune the volume fraction *in situ* [111, 352]. This feature has already been exploited in ageing experiments (see section 4.2).

One can also use sticky colloidal particles to study colloidal gelation. The most common way to induce gelation is to add a small polymer molecule to the colloidal suspension. A colloidal particle surrounded by small polymers feels an isotropic osmotic pressure whereas two particles close together feel an unbalanced osmotic pressure that pushes them together. The result is an effective attractive interaction between the particles, which has been termed the depletion force [135, 419]. The range of this interaction is set by the size of the small polymers (typically their radius of gyration is at least ten times smaller than the colloidal particle radius), and the strength of the interaction is set by the polymer concentration.

MCT made intriguing predictions of a re-entrant glass transition for hard spheres with a very short range depletion attraction [1, 420–423], with supporting evidence from simulations [424]. A fascinating set of experiments confirmed these predictions [256–259, 407, 425, 426]. A state diagram is shown in figure 17: the filled symbols indicate glassy states. The re-entrant glass transition can be understood by considering the two types of glasses. At high polymer concentration, all of the colloidal particles stick together in a gel—an 'attractive glass'—indicated by the filled squares in figure 17. Within the gel, particles are at a high local volume fraction, whereas the pores of the gel are at a lower local volume fraction [427]. If the polymer concentration is decreased, at some point, particles detach from the gelled phase and rearrange, passing through the pores, and the sample becomes ergodic: that is, a fluid! These states are shown by the inverted triangles in figure 17, and eventually these samples all crystallized. If the polymer concentration is further decreased, the distinction between the gel and the pores is lost, and the system can become glassy again—a 'repulsive glass'—indicated by the filled circles in figure 17. At this point, it is like the hard-sphere glass transition, where particle arrest is due to cages. Here the sample is much more isotropic, with the local volume fraction essentially constant and larger than $\phi_{\rm g}$. The intermediate fluid state allows for the possibility of high-volume fraction colloids with moderately low viscosities [407, 260].

For more about the physics of colloid-polymer mixtures, two classic articles are [428, 429] and good reviews are [1, 430, 431]. Microscopy studies of particle motion comparing attractive and repulsive glasses include [288, 289]. Note that for very strong attractive forces and lower volume fractions, the sample is considered a colloidal gel rather than an attractive colloidal glass; the distinction is clarified in [408].

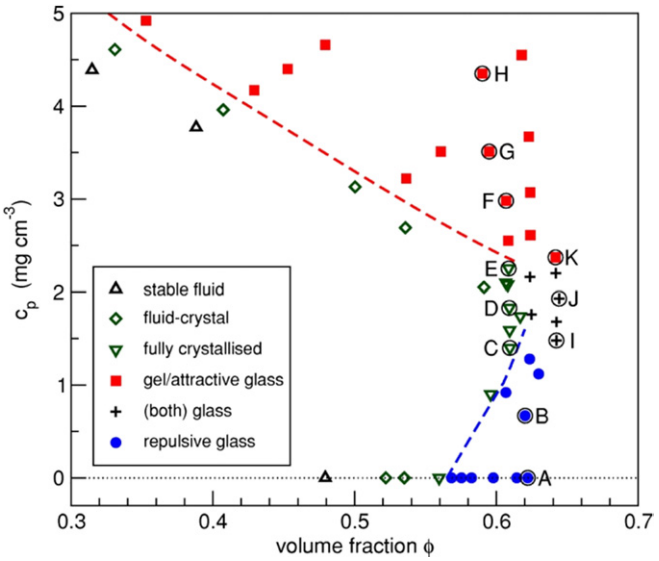

Figure 17. Phase diagram showing equilibrium and non-equilibrium states of a colloid-polymer mixture. Open symbols fully equilibrated, while filled symbols did not and thus correspond to the glassy states. The dashed curves are guides to the eye. c_p is the concentration of the added polymer, which had a size ratio (polymer radius of gyration to particle size) of $\xi = 0.09$. (The letters indicate specific states discussed in [426].) Reprinted with permission from [426], copyright 2004 by the American Physical Society.

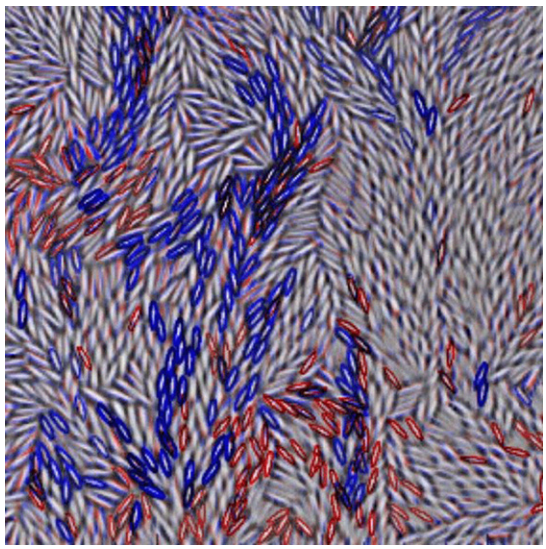

Figure 18. Ellipsoidal particles in a quasi-2D experiment. The ellipsoids that translate the most at this moment are outlined in blue (thick darker grey lines), and those that rotate the most are outlined in red (thin lighter grey lines). Those outlined in black translate and rotate. The ellipsoids are 3.33 μm long. Reprinted with permission from [472], copyright 2011 by the American Physical Society (adapted from original image in [466]).

A more exotic colloid is laponite: nanometre-sized colloidal clay platelets. These aqueous suspensions have been observed to become viscous at very low solid concentrations [432, 433] and exhibit a glass transition at remarkably low volume fractions of $\phi \approx 0.01$–0.02 [164, 434–436]. Along with rheology techniques, it is possible at such low concentrations to use DLS to study dynamics. One can also shear the suspension quickly to create highly reproducible initial liquid states. Given these advantages, laponite suspensions are commonly used in studies of ageing, in particular [343, 357, 372, 373, 375, 434, 435, 437, 438]. Many of these studies also relate to effective temperatures during ageing; see section 4.2 for more discussion of effective temperatures.

Emulsions are composed of droplets of one liquid immersed in a second immiscible liquid. The interfaces between the liquids are stabilized by surfactants; review articles discussing emulsions include [439, 440]. The emulsion glass transition appears to be closer to random close-packing [441, 442]. Emulsion glasses were recently used to study the forces between droplets in close-packed samples [443–445] and the structure of random close packing of polydisperse samples [446, 447].

Foams, bubbles of gas in a liquid, are yet another system that exhibits glassy behaviour [448, 449]. A common technique uses shear to study how the behaviour within the foam depends on shear rate. Shear in this case is used to "unjam" the foam, in contrast to increasing temperature to liquefy a glass or decreasing the volume fraction to unjam a colloidal glass. This method has been used to good effect [450–457]. One particularly thought-provoking simulation examined several different measures of an effective temperature of a sheared foam and found good agreement between the different measures [366]; see section 4.2 of this review for further discussion of effective temperatures.

Spin glasses, not yet mentioned in this review, are another large category of glass-forming systems [458]. There, glassy behaviour is controlled by range of interaction and the coupling strength between spins. It has been demonstrated that confocal microscopy observations of colloidal glasses can be mapped onto spin glass formalism [459].

5.2. *Future directions: anisotropic colloidal particles*

In recent years, a number of new methods have been successful in synthesizing non-spherical colloidal particles [460–463]. Several of these methods can produce particles suitable for colloidal glass studies; see, for example, [464, 465]. Anisotropic particles are potentially better able to mimic the molecular glass transition, which in many cases occurs with non-spherically symmetric molecules. A recent experiment studied the glass transition of colloidal ellipsoids in two dimensions [466] and found that rotational motions ceased—became glassy—at an area fraction lower than that for the translational motion. This confirmed theoretical predictions [1, 467]. An image adapted from their experimental data is shown in figure 18, indicating that these particles rotate and translate in spatially dynamically heterogeneous ways (see section 3.3). Large translational motions typically occurred for particles within aligned domains, while the large rotation motions were more prevalent between the domains. This sort of experiment could easily test other predictions: for example, simulations and theory predict a non-monotonic dependence on aspect ratio [468–470]. The differing glass transitions for rotational and translational motions should disappear for aspect

ratios closer to 1 [467, 471]. Aspect ratios closer to 1 might be useful to study, given that molecular glasses only have a single glass transition [472].

Other possibilities including using 'patchy' colloids, which have attractive regions on their surfaces. Simulations suggest interesting gel phases can form [473, 474]. A good review of experimental efforts to create patchy colloids and recent simulation results is [475].

A different take on breaking spherical symmetry is to use particles which are optically asymmetric, but spherical in other respects. Such particles have been created and their rotational motion can be tracked [476]. This is a fun technique, but probably needs to be combined with other techniques to give such particles some other non-spherical symmetry; otherwise, the spheres are unlikely to dramatically change their behaviour near the colloidal glass transition. While hydrodynamic interactions with nearby particles slow rotational motion, the regular colloidal glass transition, which is an inhibition of translational motion, would be unaffected.

The many other ways to make non-spherically symmetric particles are comprehensively reviewed in [477]. One could imagine, for example, tetrahedral particles with two sticky patches, perhaps with the sticky patches having some specified position on the tetrahedra. Studying the interplay of shape, interaction and the colloidal glass transition is likely to be fruitful for quite some time.

6. Conclusion

Colloidal suspensions are used in many ways to study the physics of the glass transition, as has been described throughout this review. As noted in the introduction, dense colloidal suspensions have material properties of potential interest and relevance to a variety of industrial processes, and so even without a connection to the glass transition, dense colloids are worthy of study. Aspects of the colloidal glass transition remain to be understood, such as the exact roles of gravity and polydispersity in suppressing crystallization, correlations between structure and dynamics, and the best way to define ϕ_g, among others. Given the rich physics in these systems and recent progress in synthesis techniques, the field is likely to continue flourishing for some time.

We consider a final pair of questions: how relevant are colloids as a model for the glass transition; and what is currently the 'best' value of ϕ_g? From the perspective of this review, the answer to the first question is clearly 'yes': the colloidal glass transition has numerous similarities to glass transitions in general and is therefore a good model system. Microscopic relaxation time scales in colloids grow dramatically (figures 2, 5 and 10), as does the macroscopic viscosity (figure 8). Colloidal glasses demonstrate an apparent variety of fragilities as shown in figure 11, although section 3.2 discusses the variety of interpretations that are possible for these data. Dense colloidal liquids exhibit spatially heterogeneous dynamics (figures 12 and 13) similar to molecular glasses, and the structure of colloidal glasses is amorphous (figure 14), similar to results from glassy simulations and molecular experiments. Colloidal glasses also exhibit ageing behaviour (figure 15) similar to molecular glasses, even matching in many details [352]. In general, results from colloids agree with glass transition theories qualitatively (figure 18) and often quantitatively (figures 5, 8 and 10).

The answer to our second question, concerning the 'best' value for ϕ_g, is one of two candidates: the traditional value $\phi_g \approx 0.58$; and the value for random close packing, $\phi_{rcp} \approx 0.64$. Much of the data mentioned above has quantities diverging at 0.58 (figures 2, 5 and 10) or changing qualitatively at 0.58 (figures 13 and 15). There is one non-trivial exception: the viscosity data in figure 8 are well fit by a function diverging at 0.64 [221]. While Cheng *et al* were only able to measure a change in viscosity of four orders of magnitude, far less than is seen for molecular glasses, it is conceivable that the experimental $\phi_g \approx 0.58$ is still below a truer glass transition point for colloids—perhaps at a volume fraction comparable to ϕ_{rcp}. The limitations of measuring larger viscosities are discussed in section 3.1.

However, volume fraction measurements are thought to have uncertainties of at least $\pm 3\%$, which possibly lowers the divergence point of [221] from 0.64 to 0.62; the specific case of the data in [221] is discussed in [66]. A second possibility is simply to accept that the viscosity at ϕ_g, while 'large,' is still finite. The same is true for the viscosities of molecular glasses at T_g, albeit at significantly larger values. Given the number of observations pointing to a glass transition at $\phi_g \approx 0.58$ as well as complementary simulation results [43, 44], we feel that 0.58 is still a reasonable 'best' candidate for ϕ_g, although it is clear that there are important questions about this value that still remain (both for viscosity [221] and relaxation times [261, 262]). It is certainly likely that the value $\phi_g \approx 0.58$, and indeed the existence of a glass transition in general, hinges on having a polydisperse sample [43, 44]—which is easy to achieve in many experiments.

Over the volume fraction range for which samples can be equilibrated ($\phi \lesssim 0.6$), colloids share many similarities with molecular glasses, both in experiments and simulations (as described above). These similarities strengthen the utility of the colloidal model system, despite the relatively limited viscosity range that is observable. Simulations are also somewhat limited in the time scales that they can address [219]. As noted in section 2.6, the agreement between colloidal experiments and computational simulations strengthens the validity of both. At this point in time, 26 years after the first experimental demonstration of the colloidal hard-sphere glass transition by Pusey and van Megen [30], many points of similarity between the colloidal glass transition at ϕ_g and the molecular glass transition have been found and studied. Thus, to answer our first question once more: colloidal glasses are indeed a useful model for understanding the glass transition.

Throughout this review, we have pointed out earlier sources where topics are discussed in more detail, and so we conclude by noting prior reviews of the colloidal glass transition, of which several have already been referenced here [1, 49, 72, 431, 478].

Acknowledgments

We thank R Besseling, L Berthier, P M Chaikin, A J Liu, D Reichman and C B Roth for helpful discussions. This work was supported by a grant from the National Science Foundation (CHE-0910707).

References

[1] Sciortino F and Tartaglia P 2005 *Adv. Phys.* **54** 471–524
[2] Götze W and Sjögren L 1992 *Rep. Prog. Phys.* **55** 241–376
[3] Angell C A 1995 *Science* **267** 1924–35
[4] Stillinger F H 1995 *Science* **267** 1935–9
[5] Ediger M D, Angell C A and Nagel S R 1996 *J. Phys. Chem.* **100** 13200–12
[6] Angell C A 2000 *J. Phys.: Condens. Matter* **12** 6463–75
[7] Debenedetti P G and Stillinger F H 2001 *Nature* **410** 259–67
[8] Andersen H C 2005 *Proc. Natl Acad. Sci. USA* **102** 6686–91
[9] Dyre J C 2006 *Rev. Mod. Phys.* **78** 953–72
[10] Berthier L and Biroli G 2011 *Rev. Mod. Phys.* **83** 587–645
[11] Roland C, Hensel-Bielowka S, Paluch M and Casalini R 2005 *Rep. Prog. Phys.* **68** 1405–78
[12] Win K Z and Menon N 2006 *Phys. Rev.* E **73** 040501
[13] Lindsay H M and Chaikin P M 1982 *J. Chem. Phys.* **76** 3774–81
[14] Zanotto E D 1998 *Am. J. Phys.* **66** 392–5
[15] Zanotto E D and Gupta P K 1999 *Am. J. Phys.* **67** 260–2
[16] Edgeworth R, Dalton B J and Parnell T 1984 *Euro. J. Phys.* **5** 198–200
[17] Vincent B 2005 *Introduction to Colloidal Dispersions* (Oxford: Blackwell) chapter 1
[18] Larson R G 1998 *The Structure and Rheology of Complex Fluids* (Oxford: Oxford University Press)
[19] Hiltner P A and Krieger I M 1969 *J. Phys. Chem.* **73** 2386–9
[20] Hiltner P A, Papir Y S and Krieger I M 1971 *J. Phys. Chem.* **75** 1881–6
[21] Kose A, Ozaki M, Takano K, Kobayashi Y and Hachisu S 1973 *J. Colloid Interface Sci.* **44** 330–8
[22] Hastings R 1978 *J. Chem. Phys.* **68** 675–8
[23] Aastuen D J W, Clark N A, Cotter L K and Ackerson B J 1986 *Phys. Rev. Lett.* **57** 1733–6
[24] Van Winkle D H and Murray C A 1986 *Phys. Rev.* A **34** 562–73
[25] Murray C A and Van Winkle D H 1987 *Phys. Rev. Lett.* **58** 1200–3
[26] Sirota E B, Yang H D O, Sinha S K, Chaikin P M, Axe J D and Fujii Y 1989 *Phys. Rev. Lett.* **62** 1524–7
[27] Murray C A, Sprenger W O and Wenk R A 1990 *Phys. Rev.* B **42** 688–703
[28] Marshall L and Zukoski C F 1990 *J. Phys. Chem.* **94** 1164–71
[29] Murray C A and Grier D G 1996 *Annu. Rev. Phys. Chem.* **47** 421–62
[30] Pusey P N and van Megen W 1986 *Nature* **320** 340–2
[31] Rosenberg R O, Thirumalai D and Mountain R D 1989 *J. Phys.: Condens. Matter* **1** 2109–14
[32] Pusey P N and van Megen W 1987 *Phys. Rev. Lett.* **59** 2083–6
[33] Pusey P N 1987 *J. Physique* **48** 709–12
[34] Bernal J D 1964 *Proc. R. Soc. Lond.* A **280** 299–322
[35] Löwen H 2000 *Fun with Hard Spheres* vol 554 (Berlin: Springer) pp 295–331
[36] Donev A, Stillinger F H and Torquato S 2007 *J. Chem. Phys.* **127** 124509
[37] Wood W W and Jacobson J D 1957 *J. Chem. Phys.* **27** 1207–8
[38] Alder B J and Wainwright T E 1957 *J. Chem. Phys.* **27** 1208–9
[39] Hoover W G and Ree F H 1967 *J. Chem. Phys.* **47** 4873–8
[40] Bolhuis P G and Kofke D A 1996 *Phys. Rev.* E **54** 634–43
[41] Auer S and Frenkel D 2001 *Nature* **413** 711–13
[42] Schöpe H J, Bryant G and van Megen W 2007 *J. Chem. Phys.* **127** 084505
[43] Zaccarelli E, Valeriani C, Sanz E, Poon W C K, Cates M E and Pusey P N 2009 *Phys. Rev. Lett.* **103** 135704
[44] Pusey P N, Zaccarelli E, Valeriani C, Sanz E, Poon W C K and Cates M E 2009 *Phil. Trans. R. Soc. Lond.* A **367** 4993–5011
[45] Fasolo M and Sollich P 2003 *Phys. Rev. Lett.* **91** 068301
[46] Sollich P and Wilding N B 2010 *Phys. Rev. Lett.* **104** 118302
[47] Hynninen A P and Dijkstra M 2003 *Phys. Rev.* E **68** 021407
[48] Hernández-Guzmán J and Weeks E R 2009 *Proc. Natl Acad. Sci. USA* **106** 15198–202
[49] Härtl W 2001 *Curr. Opin. Colloid Interface Sci.* **6** 479–83
[50] Bernal J D and Mason J 1960 *Nature* **188** 910–11
[51] Torquato S, Truskett T M and Debenedetti P G 2000 *Phys. Rev. Lett.* **84** 2064–7
[52] Radin C 2008 *J. Stat. Phys.* **131** 567–73
[53] Hermes M and Dijkstra M 2010 *Europhys. Lett.* **89** 38005
[54] Snook I, van Megen W and Pusey P 1991 *Phys. Rev.* A **43** 6900–7
[55] Speedy R J 1998 *Mol. Phys.* **95** 169–78
[56] Doliwa B and Heuer A 1998 *Phys. Rev. Lett.* **80** 4915–18
[57] Németh Z T and Löwen H 1999 *Phys. Rev.* E **59** 6824–9
[58] Foffi G, Götze W, Sciortino F, Tartaglia P and Voigtmann T 2004 *Phys. Rev.* E **69** 011505
[59] Xu N, Haxton T K, Liu A J and Nagel S R 2009 *Phys. Rev. Lett.* **103** 245701
[60] Bryant G, Williams S R, Qian L, Snook I K, Perez E and Pincet F 2002 *Phys. Rev.* E **66** 060501
[61] Underwood S M, Taylor J R and van Megen W 1994 *Langmuir* **10** 3550–4
[62] Antl L, Goodwin J W, Hill R D, Ottewill R H, Owens S M, Papworth S and Waters J A 1986 *Colloids Surf.* **17** 67–78
[63] Bosma G, Pathmamanoharana C, de Hooga E H A, Kegel W K, van Blaaderen A and Lekkerkerker H N W 2002 *J. Colloid Interface Sci.* **245** 292–300
[64] Campbell A I and Bartlett P 2002 *J. Colloid Interface Sci.* **256** 325–30
[65] Elsesser M T and Hollingsworth A D 2010 *Langmuir* **26** 17989–96
[66] Poon W C K, Weeks E R and Royall C P 2012 *Soft Matter* **8** 21–30
[67] Dinsmore A D, Weeks E R, Prasad V, Levitt A C and Weitz D A 2001 *App. Opt.* **40** 4152–9
[68] Simeonova N B and Kegel W K 2004 *Phys. Rev. Lett.* **93** 035701
[69] Zhu J, Li M, Rogers R, Meyer W, Ottewill R H, STS-73 Space Shuttle Crew, Russel W B and Chaikin P M 1997 *Nature* **387** 883–5
[70] Kegel W K 2000 *Langmuir* **16** 939–41
[71] Bartsch E 1998 *Curr. Opin. Colloid Interface Sci.* **3** 577–85
[72] Schweizer K S and Yatsenko G 2007 *J. Chem. Phys.* **127** 164505
[73] Di Cola E, Moussaïd A, Sztucki M, Narayanan T and Zaccarelli E 2009 *J. Chem. Phys.* **131** 144903
[74] Gleim T, Kob W and Binder K 1998 *Phys. Rev. Lett.* **81** 4404–7
[75] Szamel G and Flenner E 2004 *Europhys. Lett.* **67** 779–85
[76] Tokuyama M, Yamazaki H and Terada Y 2003 *Phys. Rev.* E **67** 062403
[77] Tokuyama M 2007 *Physica* A **378** 157–66
[78] Berthier L, Biroli G, Bouchaud J P, Kob W, Miyazaki K and Reichman D R 2007 *J. Chem. Phys.* **126** 184503
[79] Höfling F, Munk T, Frey E and Franosch T 2008 *J. Chem. Phys.* **128** 164517
[80] Puertas A M 2010 *J. Phys.: Condens. Matter* **22** 104121

[81] Henderson S I, Mortensen T C, Underwood S M and van Megen W 1996 *Physica* A **233** 102–16
[82] Henderson S I and van Megen W 1998 *Phys. Rev. Lett.* **80** 877–80
[83] Kob W and Andersen H C 1995 *Phys. Rev.* E **51** 4626–41
[84] Kob W and Andersen H C 1995 *Phys. Rev.* E **52** 4134–53
[85] Meller A and Stavans J 1992 *Phys. Rev. Lett.* **68** 3646–9
[86] Sutherland W 1905 *Phil. Mag.* **9** 781–5
[87] Einstein A 1905 *Ann. Phys., Lpz.* **17** 549–60
[88] Pusey P N and Tough R J A 1983 *Faraday Discuss. Chem. Soc.* **76** 123–36
[89] Snook I, van Megen W and Tough R J A 1983 *J. Chem. Phys.* **78** 5825–36
[90] Beenakker C W J and Mazur P 1983 *Phys. Lett.* A **98** 22–4
[91] Beenakker C W J and Mazur P 1984 *Physica* A **126** 349–70
[92] van Megen W, Ottewill R H, Owens S M and Pusey P N 1985 *J. Chem. Phys.* **82** 508–15
[93] Berne B J, Boon J P and Rice S A 1966 *J. Chem. Phys.* **45** 1086–96
[94] Sjögren L 1980 *Phys. Rev.* A **22** 2883–90
[95] Wahnstrom G and Sjögren L 1982 *J. Phys. C: Solid State Phys.* **15** 401
[96] Rabani E, Gezelter J D and Berne B J 1997 *J. Chem. Phys.* **107** 6867–76
[97] Verberg R, Schepper I M D and Cohen E G D 1999 *Europhys. Lett.* **48** 397–402
[98] Schweizer K S and Saltzman E J 2003 *J. Chem. Phys.* **119** 1181–96
[99] Weeks E R and Weitz D A 2002 *Chem. Phys.* **284** 361–7
[100] van Megen W, Mortensen T C, Williams S R and Müller J 1998 *Phys. Rev.* E **58** 6073–85
[101] Batchelor G K 1972 *J. Fluid Mech.* **52** 245–68
[102] Paulin S E and Ackerson B J 1990 *Phys. Rev. Lett.* **64** 2663–6
[103] He P, Mejia A F, Cheng Z, Sun D, Sue H J, Dinair D S and Marquez M 2010 *Phys. Rev.* E **81** 026310
[104] Bartsch E, Antonietti M, Schupp W and Sillescu H 1992 *J. Chem. Phys.* **97** 3950–63
[105] Bartsch E, Frenz V, Baschnagel J, Schärtl W and Sillescu H 1997 *J. Chem. Phys.* **106** 3743–56
[106] Cavagna A 2009 *Phys. Rep.* **476** 51–124
[107] Haw M D 2002 *J. Phys.: Condens. Matter* **14** 7769–79
[108] Olafsen J (ed) 2010 *Experimental and Computational Techniques in Soft Condensed Matter Physics* 1st edn (Cambridge: Cambridge University Press)
[109] Elliot M and Poon W C K 2001 *Adv. Colloid Interface Sci.* **92** 133–194
[110] Marcus A H, Schofield J and Rice S A 1999 *Phys. Rev.* E **60** 5725–36
[111] Yunker P, Zhang Z, Aptowicz K and Yodh A G 2009 *Phys. Rev. Lett.* **103** 115701
[112] König H, Hund R, Zahn K and Maret G 2005 *Eur. Phys. J.* E **18** 287–93
[113] Ebert F, Dillmann P, Maret G and Keim P 2009 *Rev. Sci. Instrum.* **80** 083902
[114] Royall C P, Leunissen M E and Blaaderen A V 2003 *J. Phys.: Condens. Matter* **15** S3581–96
[115] Yethiraj A and van Blaaderen A 2003 *Nature* **421** 513–17
[116] Yethiraj A 2007 *Soft Matter* **3** 1099–115
[117] Inoué S and Spring K R 1997 *Video Microscopy : The Fundamentals (The Language of Science)* 2nd edn (Berlin: Springer)
[118] Habdas P and Weeks E R 2002 *Curr. Opin. Colloid Interface Sci.* **7** 196–203
[119] Prasad V, Semwogerere D and Weeks E R 2007 *J. Phys.: Condens. Matter* **19** 113102
[120] Draaijer A and Houpt P M 1988 *Scanning* **10** 139–45
[121] Awamura D, Ode T and Yonezawa M 1990 *Science on Form: 3D Dynamic Morphometry for Bridge between Structure and Function, Proc. 2nd Int. Symp. for Science on Form* ed S Ishizaka (Tokyo: KTK Scientific Publishers) pp 81–95
[122] Xiao G Q, Corle T R and Kino G S 1988 *Appl. Phys. Lett.* **53** 716–18
[123] Yoshida H, Ito K and Ise N 1991 *Phys. Rev.* B **44** 435–8
[124] van Blaaderen A, Imhof A, Hage W and Vrij A 1992 *Langmuir* **8** 1514–7
[125] Ito K, Yoshida H and Ise N 1994 *Science* **263** 66–8
[126] van Blaaderen A 1993 *Adv. Mater.* **5** 52–4
[127] van Blaaderen A and Wiltzius P 1995 *Science* **270** 1177–9
[128] Kegel W K and van Blaaderen A 2000 *Science* **287** 290–3
[129] Weeks E R, Crocker J C, Levitt A C, Schofield A and Weitz D A 2000 *Science* **287** 627–31
[130] Chestnut M H 1997 *Curr. Opin. Colloid Interface Sci.* **2** 158–61
[131] Pawley J 2006 *Handbook of Biological Confocal Microscopy* 3rd edn (Berlin: Springer)
[132] Crocker J C and Grier D G 1996 *J. Colloid Interface Sci.* **179** 298–310
[133] Gao Y and Kilfoil M L 2009 *Opt. Express* **17** 4685–704
[134] Jenkins M C and Egelhaaf S U 2008 *Adv. Colloid Interface Sci.* **136** 65–92
[135] Crocker J C, Matteo J A, Dinsmore A D and Yodh A G 1999 *Phys. Rev. Lett.* **82** 4352–5
[136] Baumgartl J and Bechinger C 2005 *Europhys. Lett.* **71** 487–93
[137] Weeks E R and Weitz D A 2002 *Phys. Rev. Lett.* **89** 095704
[138] Weeks E R and Crocker J C 2012 Particle tracking using IDL http://www.physics.emory.edu/∼weeks/idl/
[139] Besseling R, Isa L, Weeks E R and Poon W C K 2009 *Adv. Colloid Interface Sci.* **146** 1–17
[140] Berne B J and Pecora R 1976 *Dynamic Light Scattering* (New York: Wiley)
[141] Jones R B and Pusey P N 1991 *Annu. Rev. Phys. Chem.* **42** 137–69
[142] van Megen W, Underwood S M and Snook I 1986 *J. Chem. Phys.* **85** 4065–72
[143] Williams S R and van Megen W 2001 *Phys. Rev.* E **64** 041502
[144] Hoffman R L 1992 *J. Rheol.* **36** 947–65
[145] D'Haene P and Mewis J 1994 *Rheol. Acta* **33** 165–74
[146] Lynch J M, Cianci G C and Weeks E R 2008 *Phys. Rev.* E **78** 031410
[147] Götze W and Voigtmann T 2003 *Phys. Rev.* E **67** 021502
[148] Foffi G, Götze W, Sciortino F, Tartaglia P and Voigtmann T 2003 *Phys. Rev. Lett.* **91** 085701
[149] Zaccarelli E, Löwen H, Wessels P P F, Sciortino F, Tartaglia P and Likos C N 2004 *Phys. Rev. Lett.* **92** 225703
[150] Pusey P N and van Megen W 1989 *Physica* A **157** 705–41
[151] Cipelletti L and Ramos L 2002 *Curr. Opin. Colloid Interface Sci.* **7** 228–34
[152] Scheffold F and Cerbino R 2007 *Curr. Opin. Colloid Interface Sci.* **12** 50–7
[153] Pusey P 1999 *Curr. Opin. Colloid Interface Sci.* **4** 177–85
[154] Maret G and Wolf P E 1987 *Z. Phys.* B **65** 409–13
[155] Wolf P E, Maret G, Akkermans E and Maynard R 1988 *J. Physique* **49** 63–75
[156] Akkermans E, Wolf P E, Maynard R and Maret G 1988 *J. Physique* **49** 77–98
[157] Pine D J, Weitz D A, Chaikin P M and Herbolzheimer E 1988 *Phys. Rev. Lett.* **60** 1134–7
[158] Pine D J, Weitz D A, Zhu J X and Herbolzheimer E 1990 *J. Physique* **51** 2101–27
[159] Maret G 1997 *Curr. Opin. Colloid Interface Sci.* **2** 251–7
[160] Klein R and Nägele G 1996 *Curr. Opin. Colloid Interface Sci.* **1** 4–10
[161] Bhatia S 2005 *Curr. Opin. Colloid Interface Sci.* **9** 404–11
[162] Berthier L, Biroli G, Bouchaud J P, Cipelletti L and van Saarloos W 2011 *Dynamical Heterogeneities in Glasses, Colloids, and Granular Media (International Series of*

Monographs on Physics) (Oxford: Oxford University Press)
[163] Mason T G and Weitz D A 1995 *Phys. Rev. Lett.* **75** 2770–3
[164] Mohan P H and Joshi Y M 2010 *Soft Matter* **6** 1462–6
[165] Puertas A M, Zaccarelli E and Sciortino F 2005 *J. Phys.: Condens. Matter* **17** L271–L277
[166] Pham K N, Petekidis G, Vlassopoulos D, Egelhaaf S U, Pusey P N and Poon W C K 2006 *Europhys. Lett.* **75** 624–30
[167] Conrad J C, Dhillon P P, Weeks E R, Reichman D R and Weitz D A 2006 *Phys. Rev. Lett.* **97** 265701
[168] de Schepper I M, Smorenburg H E and Cohen E G D 1993 *Phys. Rev. Lett.* **70** 2178–81
[169] Mason T G and Weitz D A 1995 *Phys. Rev. Lett.* **74** 1250–3
[170] Mason T G, Ganesan K, van Zanten J H, Wirtz D and Kuo S C 1997 *Phys. Rev. Lett.* **79** 3282–5
[171] Crocker J C, Valentine M T, Weeks E R, Gisler T, Kaplan P D, Yodh A G and Weitz D A 2000 *Phys. Rev. Lett.* **85** 888–91
[172] Breedveld V and Pine D J 2003 *J. Mater. Sci.* **38** 4461–70
[173] Waigh T A 2005 *Rep. Prog. Phys.* **68** 685–742
[174] Habdas P, Schaar D, Levitt A C and Weeks E R 2004 *Europhys. Lett.* **67** 477–83
[175] Squires T M and Brady J F 2005 *Phys. Fluids* **17** 073101
[176] Carpen I C and Brady J F 2005 *J. Rheol.* **49** 1483–502
[177] Drocco J A, Hastings M B, Reichhardt C J O and Reichhardt C 2005 *Phys. Rev. Lett.* **95** 088001
[178] Williams S R and Evans D J 2006 *Phys. Rev. Lett.* **96** 015701
[179] Meyer A, Marshall A, Bush B G and Furst E M 2006 *J. Rheol.* **50** 77–92
[180] Reichhardt C and Reichhardt C J O 2006 *Phys. Rev. Lett.* **96** 028301
[181] Zangi R, Mackowiak S A and Kaufman L J 2007 *J. Chem. Phys.* **126** 104501
[182] Gazuz I, Puertas A M, Voigtmann T and Fuchs M 2009 *Phys. Rev. Lett.* **102** 248302
[183] Khair A S and Squires T M 2010 *Phys. Rev. Lett.* **105** 156001
[184] Wilson L G, Harrison A W, Poon W C K and Puertas A M 2011 *Europhys. Lett.* **93** 58007
[185] Bergenholtz J 2001 *Curr. Opin. Colloid Interface Sci.* **6** 484–8
[186] Lionberger R A and Russel W B 2000 *Adv. Chem. Phys.* **111** 399–474
[187] Stickel J J and Powell R L 2005 *Annu. Rev. Fluid Mech.* **37** 129–49
[188] Buscall R 2010 *J. Rheol.* **54** 1177–83
[189] Brader J M 2010 *J. Phys.: Condens. Matter* **22** 363101
[190] Macosko C W 1994 *Rheology: Principles, Measurements, and Applications (Advances in Interfacial Engineering)* 1st edn (New York: Wiley)
[191] Jones R A L 2002 *Soft Condensed Matter* (*Oxford Master Series in Condensed Matter Physics* vol 6) 1st edn (Oxford: Oxford University Press)
[192] Chen D T N, Wen Q, Janmey P A, Crocker J C and Yodh A G 2010 *Annu. Rev. Condens. Matter Phys.* **1** 301–22
[193] Brady J F and Bossis G 1988 *Annu. Rev. Fluid Mech.* **20** 111–57
[194] Kob W, Donati C, Plimpton S J, Poole P H and Glotzer S C 1997 *Phys. Rev. Lett.* **79** 2827–30
[195] Poole P H, Donati C and Glotzer S C 1998 *Physica* A **261** 51–9
[196] Donati C, Glotzer S C and Poole P H 1999 *Phys. Rev. Lett.* **82** 5064–7
[197] Berthier L 2004 *Phys. Rev.* E **69** 020201(R)
[198] Doliwa B and Heuer A 2000 *Phys. Rev.* E **61** 6898–908
[199] Hurley M M and Harrowell P 1995 *Phys. Rev.* E **52** 1694–8
[200] Hurley M M and Harrowell P 1996 *J. Chem. Phys.* **105** 10521–6
[201] Yamamoto R and Onuki A 1998 *Phys. Rev.* E **58** 3515–29
[202] Kurita R and Weeks E R 2010 *Phys. Rev.* E **82** 041402
[203] Widmer-Cooper A, Harrowell P and Fynewever H 2004 *Phys. Rev. Lett.* **93** 135701
[204] Donati C, Douglas J F, Kob W, Plimpton S J, Poole P H and Glotzer S C 1998 *Phys. Rev. Lett.* **80** 2338–41
[205] Kasper A, Bartsch E and Sillescu H 1998 *Langmuir* **14** 5004–10
[206] van Meel J A, Frenkel D and Charbonneau P 2009 *Phys. Rev.* E **79** 030201(R)
[207] van Meel J A, Charbonneau B, Fortini A and Charbonneau P 2009 *Phys. Rev.* E **80** 061110
[208] Charbonneau P, Ikeda A, van Meel J A and Miyazaki K 2010 *Phys. Rev.* E **81** 040501(R)
[209] Kob W, Scheidler P and Binder K 2000 *Europhys. Lett.* **52** 277–83
[210] Kim K and Yamamoto R 2000 *Phys. Rev.* E **61** R41–4
[211] Murray C 1998 *MRS Bull.* **23** 33–8
[212] Archer A J, Hopkins P and Schmidt M 2007 *Phys. Rev.* E **75** 040501
[213] Nugent C R, Edmond K V, Patel H N and Weeks E R 2007 *Phys. Rev. Lett.* **99** 025702
[214] Desmond K W and Weeks E R 2009 *Phys. Rev.* E **80** 051305
[215] Edmond K V, Nugent C R and Weeks E R 2010 *Eur. Phys. J. Spec. Top.* **189** 83–93
[216] Widmer-Cooper A and Harrowell P 2005 *J. Phys.: Condens. Matter* **17** S4025–34
[217] Santen L and Krauth W 2000 *Nature* **405** 550–1
[218] Frenkel D and Smit B 2001 *Understanding Molecular Simulation, From Algorithms to Applications (Computational Science)* 2nd edn (New York: Academic)
[219] Glotzer S C 2000 *J. Non-Cryst. Solids* **274** 342–55
[220] Habdas P, Weeks E R and Lynn D G 2006 *Phys. Teach.* **44** 276–9
[221] Cheng Z, Zhu J, Chaikin P M, Phan S E and Russel W B 2002 *Phys. Rev.* E **65** 041405
[222] Crassous J J, Siebenbürger M, Ballauff M, Drechsler M, Hajnal D, Henrich O and Fuchs M 2008 *J. Chem. Phys.* **128** 204902
[223] Siebenbürger M, Fuchs M, Winter H and Ballauff M 2009 *J. Rheol.* **53** 707–26
[224] Yamamoto R and Onuki A 1997 *Europhys. Lett.* **40** 61–6
[225] Phan S E, Russel W B, Cheng Z, Zhu J, Chaikin P M, Dunsmuir J H and Ottewill R H 1996 *Phys. Rev.* E **54** 6633–45
[226] Pusey P, Segre P, Behrend O, Meeker S and Poon W 1997 *Physica* A **235** 1–8
[227] Mewis J, Frith W J, Strivens T A and Russel W B 1989 *AIChE J.* **35** 415–22
[228] Doolittle A K 1951 *J. App. Phys.* **22** 1471–5
[229] Tarjus G and Kivelson D 2001 *The Viscous Slowing Down of Supercooled Liquids and the Glass Transition: Phenomonology, Concepts, and Models* 1st edn (London: Taylor and Francis) pp 20–38
[230] Woodcock L V and Angell C A 1981 *Phys. Rev. Lett.* **47** 1129–32
[231] Hecksher T, Nielsen A I, Olsen N B and Dyre J C 2008 *Nature Phys.* **4** 737–41
[232] McKenna G B 2008 *Nature Phys.* **4** 673
[233] Olsson P and Teitel S 2007 *Phys. Rev. Lett.* **99** 178001
[234] Olsson P and Teitel S 2011 *Phys. Rev.* E **83** 030302
[235] Vaagberg D, Balderas D V, Moore M A, Olsson P and Teitel S 2011 *Phys. Rev.* E **83** 030303
[236] Ediger M D 2000 *Annu. Rev. Phys. Chem.* **51** 99–128
[237] Ngai K L and Rendell R W 1998 *Phil. Mag.* B **77** 621–31
[238] Ngai K 2007 *J. Non-Cryst. Solids* **353** 709–18

[239] Segrè P N, Meeker S P, Pusey P N and Poon W C K 1995 *Phys. Rev. Lett.* **75** 958–61
[240] Fujara F, Geil B, Sillescu H and Fleischer G 1992 *Z. Phys.* B **88** 195–204
[241] Cicerone M T and Ediger M D 1993 *J. Phys. Chem.* **97** 10489–97
[242] Chang I, Fujara F, Geil B, Heuberger G, Mangel T and Sillescu H 1994 *J. Non-Cryst. Solids* **172–174** 248–55
[243] de Schepper I M, Cohen E G D and Verberg R 1996 *Phys. Rev. Lett.* **77** 584
[244] Segrè P N, Meeker S P, Pusey P N and Poon W C K 1996 *Phys. Rev. Lett.* **77** 585
[245] Bonn D and Kegel W K 2003 *J. Chem. Phys.* **118** 2005–9
[246] Imhof A, van Blaaderen A, Maret G, Mellema J and Dhont J K G 1994 *J. Chem. Phys.* **100** 2170–81
[247] van Megen W and Underwood S M 1994 *Phys. Rev.* E **49** 4206–20
[248] van Megen W and Underwood S M 1988 *J. Chem. Phys.* **88** 7841–6
[249] van Megen W and Underwood S M 1989 *J. Chem. Phys.* **91** 552–9
[250] van Megen W and Pusey P N 1991 *Phys. Rev.* A **43** 5429–41
[251] van Megen W, Martinez V A and Bryant G 2009 *Phys. Rev. Lett.* **102** 168301
[252] Götze W and Sjögren L 1991 *Phys. Rev.* A **43** 5442–8
[253] Weysser F, Puertas A M, Fuchs M and Voigtmann T 2010 *Phys. Rev.* E **82** 011504
[254] Bartsch E, Frenz V, Moller S and Sillescu H 1993 *Physica* A **201** 363–71
[255] Bartsch E 1995 *J. Non-Cryst. Solids* **192/193** 384–92
[256] Bartsch E, Eckert T, Pies C and Sillescu H 2002 *J. Non-Cryst. Solids* **307–310** 802–11
[257] Eckert T and Bartsch E 2002 *Phys. Rev. Lett.* **89** 125701
[258] Eckert T and Bartsch E 2003 *Faraday Discuss.* **123** 51–64
[259] Eckert T and Bartsch E 2004 *J. Phys.: Condens. Matter* **16** S4937–S4950
[260] Willenbacher N, Vesaratchanon J S, Thorwarth O and Bartsch E 2011 *Soft Matter* **7** 5777–88
[261] Brambilla G, El Masri D E M, Pierno M, Berthier L, Cipelletti L, Petekidis G and Schofield A B 2009 *Phys. Rev. Lett.* **102** 085703
[262] El Masri D, Brambilla G, Pierno M, Petekidis G, Schofield A B, Berthier L and Cipelletti L 2009 *J. Stat. Mech.* **2009** P07015
[263] van Megen W and Williams S R 2010 *Phys. Rev. Lett.* **104** 169601
[264] Brambilla G, Masri D E, Pierno M, Berthier L, Cipelletti L, Petekidis G and Schofield A 2010 *Phys. Rev. Lett.* **104** 169602
[265] Reinhardt J, Weysser F and Fuchs M 2010 *Phys. Rev. Lett.* **105** 199604
[266] Brambilla G, Masri D E, Pierno M, Berthier L and Cipelletti L 2010 *Phys. Rev. Lett.* **105** 199605
[267] Tokuyama M and Oppenheim I 1994 *Phys. Rev.* E **50** R16–R19
[268] Tokuyama M and Oppenheim I 1995 *Physica* A **216** 85–119
[269] van Megen W, Martinez V A and Bryant G 2009 *Phys. Rev. Lett.* **103** 258302
[270] Reichman D R and Charbonneau P 2005 *J. Stat. Mech.* **2005** P05013
[271] Zaccarelli E, Foffi G, Gregorio P D, Sciortino F, Tartaglia P and Dawson K A 2002 *J. Phys.: Condens. Matter* **14** 2413–37
[272] Berthier L and Witten T A 2009 *Phys. Rev.* E **80** 021502
[273] Hodge I 1996 *J. Non-Cryst. Solids* **202** 164–72
[274] Martinez L M and Angell C A 2001 *Nature* **410** 663–7
[275] Huang D, Colucci D M and McKenna G B 2002 *J. Chem. Phys.* **116** 3925–34
[276] Mattsson J, Wyss H M, Fernandez-Nieves A, Miyazaki K, Hu Z, Reichman D R and Weitz D A 2009 *Nature* **462** 83–6
[277] Michele C D, Sciortino F and Coniglio A 2004 *J. Phys.: Condens. Matter* **16** L489–94
[278] Berthier L, Flenner E, Jacquin H and Szamel G 2010 *Phys. Rev.* E **81** 031505
[279] Barker J A and Henderson D 1976 *Rev. Mod. Phys.* **48** 587–671
[280] Berthier L and Witten T A 2009 *Europhys. Lett.* **86** 10001
[281] Stieger M, Pedersen J S, Lindner P and Richtering W 2004 *Langmuir* **20** 7283–92
[282] Eckert T and Richtering W 2008 *J. Chem. Phys.* **129** 124902
[283] Senff H and Richtering W 1999 *J. Chem. Phys.* **111** 1705–11
[284] Sillescu H 1999 *J. Non-Cryst. Solids* **243** 81–108
[285] Richert R 2002 *J. Phys.: Condens. Matter* **14** R703–R738
[286] Adam G and Gibbs J H 1965 *J. Chem. Phys.* **43** 139–46
[287] Mazoyer S, Ebert F, Maret G and Keim P 2009 *Europhys. Lett.* **88** 66004
[288] Kaufman L J and Weitz D A 2006 *J. Chem. Phys.* **125** 074716
[289] Latka A, Han Y, Alsayed A M, Schofield A B, Yodh A G and Habdas P 2009 *Europhys. Lett.* **86** 58001
[290] Weeks E R, Crocker J C and Weitz D A 2007 *J. Phys.: Condens. Matter* **19** 205131
[291] Courtland R E and Weeks E R 2003 *J. Phys.: Condens. Matter* **15** S359–S365
[292] Donati C, Glotzer S C, Poole P H, Kob W and Plimpton S J 1999 *Phys. Rev.* E **60** 3107–19
[293] Karmakar S, Dasgupta C and Sastry S 2009 *Proc. Natl Acad. Sci. USA* **106** 3675–9
[294] Glotzer S C, Novikov V N and Schrøder T B 2000 *J. Chem. Phys.* **112** 509–12
[295] Lačević N, Starr F W, Schrøder T B and Glotzer S C 2003 *J. Chem. Phys.* **119** 7372–87
[296] Conrad J C, Starr F W and Weitz D A 2005 *J. Phys. Chem.* B **109** 21235–40
[297] Kurita R and Weeks E R 2011 arXiv:1112.1460
[298] Matharoo G S, Razul M S G and Poole P H 2006 *Phys. Rev.* E **74** 050502
[299] Berthier L and Jack R L 2007 *Phys. Rev.* E **76** 041509
[300] Cipelletti L, Bissig H, Trappe V, Ballesta P and Mazoyer S 2003 *J. Phys.: Condens. Matter* **15** S257–62
[301] Berthier L, Chandler D and Garrahan J P 2005 *Europhys. Lett.* **69** 320–6
[302] Keys A S, Abate A R, Glotzer S C and Durian D J 2007 *Nature Phys.* **3** 260–4
[303] Berthier L, Biroli G, Bouchaud J P, Kob W, Miyazaki K and Reichman D R 2007 *J. Chem. Phys.* **126** 184504
[304] Ballesta P, Duri A and Cipelletti L 2008 *Nature Phys.* **4** 550–4
[305] Sarangapani P, Zhao J and Zhu Y 2008 *J. Chem. Phys.* **129** 104514
[306] Narumi T, Franklin S V, Desmond K W, Tokuyama M and Weeks E R 2011 *Soft Matter* **7** 1472–82
[307] Alba-Simionesco C, Coasne B, Dosseh G, Dudziak G, Gubbins K E, Radhakrishnan R and Sliwinska-Bartkowiak M 2006 *J. Phys.: Condens. Matter* **18** R15–R68
[308] Alcoutlabi M and McKenna G B 2005 *J. Phys.: Condens. Matter* **17** R461–R524
[309] Roth C B and Dutcher J R 2005 *J. Electroanal. Chem.* **584** 13–22
[310] Jackson C L and McKenna G B 1991 *J. Non-Cryst. Solids* **131–133** 221–4
[311] Barut G, Pissis P, Pelster R and Nimtz G 1998 *Phys. Rev. Lett.* **80** 3543–6
[312] Schüller J, Mel'nichenko Y, Richert R and Fischer E W 1994 *Phys. Rev. Lett.* **73** 2224–7

[313] Morineau D, Xia Y and Simionesco C A 2002 *J. Chem. Phys.* **117** 8966–72
[314] Ngai K L 2002 *Phil. Mag.* B **82** 291–303
[315] Ellison C J and Torkelson J M 2003 *Nature Mater.* **2** 695–700
[316] Priestley R D, Ellison C J, Broadbelt L J and Torkelson J M 2005 *Science* **309** 456–9
[317] Roth C B, McNerny K L, Jager W F and Torkelson J M 2007 *Macromolecules* **40** 2568–74
[318] Richert R 2011 *Annu. Rev. Phys. Chem.* **62** 65–84
[319] Bureau L 2010 *Phys. Rev. Lett.* **104** 218302
[320] Thompson P A, Grest G S and Robbins M O 1992 *Phys. Rev. Lett.* **68** 3448–51
[321] Sarangapani P S and Zhu Y 2008 *Phys. Rev.* E **77** 010501
[322] Goel G, Krekelberg W P, Errington J R and Truskett T M 2008 *Phys. Rev. Lett.* **100** 106001
[323] Mittal J, Truskett T M, Errington J R and Hummer G 2008 *Phys. Rev. Lett.* **100** 145901
[324] Kurita R and Weeks E R 2010 *Phys. Rev.* E **82** 011403
[325] Donev A, Stillinger F H and Torquato S 2005 *Phys. Rev. Lett.* **95** 090604
[326] Torquato S and Stillinger F H 2003 *Phys. Rev.* E **68** 041113
[327] Zachary C E, Jiao Y and Torquato S 2011 *Phys. Rev. Lett.* **106** 178001
[328] Zachary C E, Jiao Y and Torquato S 2011 *Phys. Rev.* E **83** 051308
[329] Berthier L, Chaudhuri P, Coulais C, Dauchot O and Sollich P 2011 *Phys. Rev. Lett.* **106** 120601
[330] Kurita R and Weeks E R 2011 *Phys. Rev.* E **84** 030401(R)
[331] Hodge I M 1995 *Science* **267** 1945–7
[332] Kob W and Barrat J L 1997 *Phys. Rev. Lett.* **78** 4581–4
[333] Kob W, Barrat J L, Sciortino F and Tartaglia P 2000 *J. Phys.: Condens. Matter* **12** 6385–94
[334] Kob W and Barrat J L 2000 *Eur. Phys. J.* B **13** 319–33
[335] Martinez V A, Bryant G and van Megen W 2008 *Phys. Rev. Lett.* **101** 135702
[336] Vollmayr-Lee K, Roman J A and Horbach J 2010 *Phys. Rev.* E **81** 061203
[337] Rottler J and Warren M 2008 *Euro. Phys. J. Spec. Top.* **161** 55–63
[338] Boettcher S and Sibani P 2011 *J. Phys.: Condens. Matter* **23** 065103
[339] Masri D E, Pierno M, Berthier L and Cipelletti L 2005 *J. Phys.: Condens. Matter* **17** S3543–S3549
[340] Castillo H E, Chamon C, Cugliandolo L F and Kennett M P 2002 *Phys. Rev. Lett.* **88** 237201
[341] Cloitre M, Borrega R and Leibler L 2000 *Phys. Rev. Lett.* **85** 4819–22
[342] Viasnoff V and Lequeux F 2002 *Phys. Rev. Lett.* **89** 065701
[343] Bonn D, Tanase S, Abou B, Tanaka H and Meunier J 2002 *Phys. Rev. Lett.* **89** 015701
[344] Derec C, Ducouret G, Ajdari A and Lequeux F 2003 *Phys. Rev.* E **67** 061403
[345] Purnomo E H, van den Ende D, Mellema J and Mugele F 2006 *Europhys. Lett.* **76** 74–80
[346] Cianci G C, Courtland R E and Weeks E R 2006 *Solid State Commun.* **139** 599–604
[347] McKenna G B 2003 *J. Phys.: Condens. Matter* **15** S737–S763
[348] McKenna G B, Narita T and Lequeux F 2009 *J. Rheol.* **53** 489–516
[349] Purnomo E H, van den Ende D, Mellema J and Mugele F 2007 *Phys. Rev.* E **76** 021404
[350] van den Ende D, Purnomo E H, Duits M H G, Richtering W and Mugele F 2010 *Phys. Rev.* E **81** 011404
[351] Purnomo E H, van den Ende D, Vanapalli S A and Mugele F 2008 *Phys. Rev. Lett.* **101** 238301
[352] Di X, Win K Z, McKenna G B, Narita T, Lequeux F, Pullela S R and Cheng Z 2011 *Phys. Rev. Lett.* **106** 095701
[353] Kovacs A J 1964 *Fortschr. Hochpolym. Forsch.* **3** 394–507
[354] Zheng Y and McKenna G B 2003 *Macromolecules* **36** 2387–96
[355] Tant M R and Wilkes G L 1981 *Polym. Eng. Sci.* **21** 874–95
[356] Cianci G C, Courtland R E and Weeks E R 2006 *AIP Conf. Proc.* **832** 21–5
[357] Buisson L, Bellon L and Ciliberto S 2003 *J. Phys.: Condens. Matter* **15** S1163–S1179
[358] Vollmayr-Lee K, Kob W, Binder K and Zippelius A 2002 *J. Chem. Phys.* **116** 5158–66
[359] Vollmayr-Lee K and Zippelius A 2005 *Phys. Rev.* E **72** 041507
[360] Castillo H E and Parsaeian A 2007 *Nature Phys.* **3** 26–8
[361] Kob W, Sciortino F and Tartaglia P 2000 *Europhys. Lett.* **49** 590–6
[362] Kawasaki T, Araki T and Tanaka H 2007 *Phys. Rev. Lett.* **99** 215701
[363] Royall C P, Williams S R, Ohtsuka T and Tanaka H 2008 *Nature Mater.* **7** 556–61
[364] Cugliandolo L F, Kurchan J and Peliti L 1997 *Phys. Rev.* E **55** 3898–914
[365] Segrè P N, Liu F, Umbanhowar P and Weitz D A 2001 *Nature* **409** 594–7
[366] Ono I K, O'Hern C S, Durian D J, Langer S A, Liu A J and Nagel S R 2002 *Phys. Rev. Lett.* **89** 095703
[367] Song C, Wang P and Makse H A 2005 *Proc. Natl Acad. Sci. USA* **102** 2299–304
[368] Wang P, Song C, Briscoe C and Makse H A 2008 *Phys. Rev.* E **77** 061309
[369] Kawasaki T and Tanaka H 2009 *Phys. Rev. Lett.* **102** 185701
[370] Grigera T S and Israeloff N E 1999 *Phys. Rev. Lett.* **83** 5038–41
[371] Hérisson D and Ocio M 2002 *Phys. Rev. Lett.* **88** 257202
[372] Bellon L 2002 *Physica* D **168/169** 325–35
[373] Bellon L, Ciliberto S and Laroche C 2001 *Europhys. Lett.* **53** 511–17
[374] Wang P, Song C and Makse H A 2006 *Nature Phys.* **2** 526–31
[375] Farouji S J, Mizuno D, Atakhorrami M, Mackintosh F C, Schmidt C F, Eiser E, Wegdam G H and Bonn D 2007 *Phys. Rev. Lett.* **98** 108302
[376] Assoud L, Ebert F, Keim P, Messina R, Maret G and Löwen H 2009 *Phys. Rev. Lett.* **102** 238301
[377] Koumakis N, Schofield A B and Petekidis G 2008 *Soft Matter* **4** 2008–18
[378] Fielding S M, Cates M E and Sollich P 2009 *Soft Matter* **5** 2378–82
[379] Rogers R B and Lagerlöf K P D 2008 *Appl. Opt.* **47** 284–95
[380] Chen D, Semwogerere D, Sato J, Breedveld V and Weeks E R 2010 *Phys. Rev.* E **81** 011403
[381] Petekidis G, Vlassopoulos D and Pusey P N 2003 *Faraday Discuss.* **123** 287–302
[382] Petekidis G, Vlassopoulos D and Pusey P N 2004 *J. Phys.: Condens. Matter* **16** S3955–S3963
[383] Eisenmann C, Kim C, Mattsson J and Weitz D A 2010 *Phys. Rev. Lett.* **104** 035502
[384] Maloney C E and Robbins M O 2008 *J. Phys.: Condens. Matter* **20** 244128
[385] Schall P, Weitz D A and Spaepen F 2007 *Science* **318** 1895–9
[386] Petekidis G, Moussaïd A and Pusey P N 2002 *Phys. Rev.* E **66** 051402
[387] Besseling R, Weeks E R, Schofield A B and Poon W C K 2007 *Phys. Rev. Lett.* **99** 028301
[388] Zausch J, Horbach J, Laurati M, Egelhaaf S U, Brader J M, Voigtmann T and Fuchs M 2008 *J. Phys.: Condens. Matter* **20** 404210
[389] Chikkadi V, Wegdam G, Bonn D, Nienhuis B and Schall P 2011 *Phys. Rev. Lett.* **107** 198303
[390] Shiba H and Onuki A 2010 *Phys. Rev.* E **81** 051501
[391] Furukawa A, Kim K, Saito S and Tanaka H 2009 *Phys. Rev. Lett.* **102** 016001

[392] Falk M L and Langer J S 1998 *Phys. Rev.* E **57** 7192–205
[393] Manneville S 2008 *Rheol. Acta* **47** 301–18
[394] Ovarlez G, Rodts S, Chateau X and Coussot P 2009 *Rheol. Acta* **48** 831–44
[395] Schall P and van Hecke M 2010 *Annu. Rev. Fluid Mech.* **42** 67–88
[396] Dhont J K G 1999 *Phys. Rev.* E **60** 4534–44
[397] Dhont J K G, Lettinga M P, Dogic Z, Lenstra T A J, Wang H, Rathgeber S, Carletto P, Willner L, Frielinghaus H and Lindner P 2003 *Faraday Discuss.* **123** 157–72
[398] Dhont J and Briels W 2008 *Rheol. Acta* **47** 257–81
[399] Moller P C F, Rodts S, Michels M A J and Bonn D 2008 *Phys. Rev.* E **77** 041507
[400] Besseling R, Isa L, Ballesta P, Petekidis G, Cates M E and Poon W C K 2010 *Phys. Rev. Lett.* **105** 268301
[401] Ballesta P, Besseling R, Isa L, Petekidis G and Poon W C K 2008 *Phys. Rev. Lett.* **101** 258301
[402] Divoux T, Tamarii D, Barentin C and Manneville S 2010 *Phys. Rev. Lett.* **104** 208301
[403] Hébraud P, Lequeux F, Munch J P and Pine D J 1997 *Phys. Rev. Lett.* **78** 4657–60
[404] Le Grand A and Petekidis G 2008 *Rheol. Acta* **47** 579–90
[405] Rogers R B and Ackerson B J 2010 *Phil. Mag.* **91** 682–729
[406] Smith P A, Petekidis G, Egelhaaf S U and Poon W C K 2007 *Phys. Rev.* E **76** 041402
[407] Pham K N, Petekidis G, Vlassopoulos D, Egelhaaf S U, Poon W C K and Pusey P N 2008 *J. Rheol.* **52** 649–76
[408] Zaccarelli E and Poon W C K 2009 *Proc. Natl Acad. Sci. USA* **106** 15203–8
[409] Sollich P, Lequeux F, Hébraud P and Cates M E 1997 *Phys. Rev. Lett.* **78** 2020–3
[410] Brader J M, Voigtmann T, Cates M E and Fuchs M 2007 *Phys. Rev. Lett.* **98** 058301
[411] Goyon J, Colin A, Ovarlez G, Ajdari A and Bocquet L 2008 *Nature* **454** 84–7
[412] Bocquet L, Colin A and Ajdari A 2009 *Phys. Rev. Lett.* **103** 036001
[413] Katgert G, Tighe B P, Möbius M E and van Hecke M 2010 *Europhys. Lett.* **90** 54002
[414] Nichol K, Zanin A, Bastien R, Wandersman E and van Hecke M 2010 *Phys. Rev. Lett.* **104** 078302
[415] Chen K, Ellenbroek W G, Zhang Z, Chen D T N, Yunker P J, Henkes S, Brito C, Dauchot O, van Saarloos W, Liu A J and Yodh A G 2010 *Phys. Rev. Lett.* **105** 025501
[416] Dingenouts N, Norhausen C and Ballauff M 1998 *Macromolecules* **31** 8912–8917
[417] Crassous J J, Wittemann A, Siebenbürger M, Schrinner M, Drechsler M and Ballauff M 2008 *Colloid Polym. Sci.* **286** 805–12
[418] Jones C D and Lyon L A 2000 *Macromolecules* **33** 8301–6
[419] Asakura S and Oosawa F 1954 *J. Chem. Phys.* **22** 1255–6
[420] Fabbian L, Götze W, Sciortino F, Tartaglia P and Thiery F 1999 *Phys. Rev.* E **59** R1347–R1350
[421] Fabbian L, Götze W, Sciortino F, Tartaglia P and Thiery F 1999 *Phys. Rev.* E **60** 2430
[422] Bergenholtz J and Fuchs M 1999 *Phys. Rev.* E **59** 5706–15
[423] Dawson K, Foffi G, Fuchs M, Götze W, Sciortino F, Sperl M, Tartaglia P, Voigtmann Th and Zaccarelli E 2000 *Phys. Rev.* E **63** 011401
[424] Puertas A M, Fuchs M and Cates M E 2002 *Phys. Rev. Lett.* **88** 098301
[425] Pham K N, Puertas A M, Bergenholtz J, Egelhaaf S U, Moussaïd A, Pusey P N, Schofield A B, Cates M E, Fuchs M and Poon W C K 2002 *Science* **296** 104–6
[426] Pham K N, Egelhaaf S U, Pusey P N and Poon W C K 2004 *Phys. Rev.* E **69** 011503
[427] Lu P J, Zaccarelli E, Ciulla F, Schofield A B, Sciortino F and Weitz D A 2008 *Nature* **453** 499–503
[428] Lekkerkerker H N W, Poon W C K, Pusey P N, Stroobants A and Warren P B 1992 *Europhys. Lett.* **20** 559–64
[429] Ilett S M, Orrock A, Poon W C K and Pusey P N 1995 *Phys. Rev.* E **51** 1344–52
[430] Poon W C K 2002 *J. Phys.: Condens. Matter* **14** R859–R880
[431] Dawson K A 2002 *Curr. Opin. Colloid Interface Sci.* **7** 218–27
[432] Mourchid A, Delville A, Lambard J, LeColier E and Levitz P 1995 *Langmuir* **11** 1942–50
[433] Mourchid A, Lécolier E, Van Damme H and Levitz P 1998 *Langmuir* **14** 4718–23
[434] Bonn D, Tanaka H, Wegdam G, Kellay H and Meunier J 1999 *Europhys. Lett.* **45** 52–7
[435] Abou B, Bonn D and Meunier J 2001 *Phys. Rev.* E **64** 021510
[436] Joshi Y M 2007 *J. Chem. Phys.* **127** 081102
[437] Bellour M, Knaebel A, Harden J L, Lequeux F and Munch J P 2003 *Phys. Rev.* E **67** 031405
[438] Bandyopadhyay R, Liang D, Yardimci H, Sessoms D A, Borthwick M A, Mochrie S G J, Harden J L and Leheny R L 2004 *Phys. Rev. Lett.* **93** 228302
[439] Bibette J, Calderon L F and Poulin P 1999 *Rep. Prog. Phys.* **62** 969–1033
[440] Mason T G, Wilking J N, Meleson K, Chang C B and Graves S M 2006 *J. Phys.: Condens. Matter* **18** R635–R666
[441] Mason T G, Bibette J and Weitz D A 1995 *Phys. Rev. Lett.* **75** 2051–4
[442] Mason T G, Lacasse M D, Grest G S, Levine D, Bibette J and Weitz D A 1997 *Phys. Rev.* E **56** 3150–66
[443] Brujić J, Edwards S F, Grinev D V, Hopkinson I, Brujic D and Makse H A 2003 *Faraday Discuss.* **123** 207–20
[444] Brujić J, Edwards S F, Hopkinson I and Makse H 2003 *Physica* A **327** 201–12
[445] Zhou J, Long S, Wang Q and Dinsmore A D 2006 *Science* **312** 1631–3
[446] Brujić J, Song C, Wang P, Briscoe C, Marty G and Makse H A 2007 *Phys. Rev. Lett.* **98** 248001
[447] Clusel M, Corwin E I, Siemens A O N and Brujić J 2009 *Nature* **460** 611–5
[448] O'Hern C S, Langer S A, Liu A J and Nagel S R 2001 *Phys. Rev. Lett.* **86** 111–4
[449] Katgert G and van Hecke M 2010 *Europhys. Lett.* **92** 34002
[450] Durian D J 1995 *Phys. Rev. Lett.* **75** 4780–3
[451] Saint-Jalmes A and Durian D J 1999 *J. Rheol.* **43** 1411–22
[452] Langer S A and Liu A J 2000 *Europhys. Lett.* **49** 68–74
[453] Debrégeas G, Tabuteau H and di Meglio J M 2001 *Phys. Rev. Lett.* **87** 178305
[454] Lauridsen J, Twardos M and Dennin M 2002 *Phys. Rev. Lett.* **89** 098303
[455] Kabla A and Debrégeas G 2003 *Phys. Rev. Lett.* **90** 258303
[456] Dennin M 2004 *Phys. Rev.* E **70** 041406
[457] Lundberg M, Krishan K, Xu N, O'Hern C S and Dennin M 2008 *Phys. Rev.* E **77** 041505
[458] Edwards S F and Anderson P W 1975 *J. Phys. F: Met. Phys.* **5** 965–74
[459] Chamon C, Cugliandolo L F, Fabricius G, Iguain J L and Weeks E R 2008 *Proc. Natl Acad. Sci. USA* **105** 15263–8
[460] Manoharan V N, Elsesser M T and Pine D J 2003 *Science* **301** 483–7
[461] Yi G R, Manoharan V N, Michel E, Elsesser M T, Yang S M and Pine D J 2004 *Adv. Mater.* **16** 1204–8
[462] Mohraz A and Solomon M J 2005 *Langmuir* **21** 5298–306
[463] Champion J A, Katare Y K and Mitragotri S 2007 *Proc. Natl Acad. Sci. USA* **104** 11901–4
[464] Gerbode S J, Lee S H, Liddell C M and Cohen I 2008 *Phys. Rev. Lett.* **101** 058302
[465] Elsesser M T, Hollingsworth A D, Edmond K V and Pine D J 2011 *Langmuir* **27** 917–27

[466] Zheng Z, Wang F and Han Y 2011 *Phys. Rev. Lett.* **107** 065702
[467] Schilling R and Scheidsteger T 1997 *Phys. Rev.* E **56** 2932–49
[468] Letz M, Schilling R and Latz A 2000 *Phys. Rev.* E **62** 5173–8
[469] Yatsenko G and Schweizer K S 2007 *Phys. Rev.* E **76** 041506
[470] De Michele C, Schilling R and Sciortino F 2007 *Phys. Rev. Lett.* **98** 265702
[471] Pfleiderer P, Milinkovic K and Schilling T 2008 *Europhys. Lett.* **84** 16003
[472] Weeks E R 2011 *Physics* **4** 61
[473] Bianchi E, Largo J, Tartaglia P, Zaccarelli E and Sciortino F 2006 *Phys. Rev. Lett.* **97** 168301
[474] Zaccarelli E 2007 *J. Phys.: Condens. Matter* **19** 323101
[475] Bianchi E, Blaak R and Likos C N 2011 *Phys. Chem. Chem. Phys.* **13** 6397–410
[476] Anthony S M, Hong L, Kim M and Granick S 2006 *Langmuir* **22** 9812–5
[477] Glotzer S C and Solomon M J 2007 *Nature Mater.* **6** 557–62
[478] Pusey P N 2008 *J. Phys.: Condens. Matter* **20** 494202